

**ANALYTICAL EVALUATION OF INORGANIC POLYMER MATERIALS FOR
INFRASTRUCTURE REPAIR**

By

ADITYA MANTHA

A thesis submitted to the

Graduate School-New Brunswick

Rutgers, The State University of New Jersey

in partial fulfillment of the requirements

for the degree of

Master of Science

Graduate Program in Civil and Environmental Engineering

written under the direction of

Dr. Husam Najm

and approved by

New Brunswick, New Jersey

October, 2014

ABSTRACT OF THE THESIS

Analytical Evaluation of Inorganic Polymer Materials for Infrastructure Repair

by ADITYA MANTHA

Thesis Director:

Dr. Husam Najm

Abstract

This thesis is an investigation of the effectiveness of repair of reinforced concrete structures with inorganic polymer compared to organic epoxy system using finite element analysis. A finite element based approach was adopted to analyze the load deformation response and the stress strain behavior of the repaired structure at the notch location due to loading. For this study ANSYS 14.5 analysis program was used as a tool to study the numerical based response of the structure. The finite element results obtained were validated by comparing the result to experimental investigations made in previous studies. A finite element model was developed to include the bond slip interaction at the steel concrete interface and the analytical results were compared to the experimental values. Detailed descriptions for the choice of elements, material data input and the solution controls input in the program are

provided in this study. The results from this study showed that the load deflection response of beam repaired with inorganic polymer is similar to the control specimens. The study also showed the effect of bond slip at the interface between steel and concrete on the load deflection response. The conclusions and recommendations of this study are mentioned for further investigation related to this study.

Acknowledgments

This research was performed under the supervision of Dr. Husam Najm. I am extremely grateful to Dr Najm for his patience, knowledge and support in helping me complete this thesis. I am grateful to Dr. P.N Balaguru for having his door open for me to listen to my questions and give advice. Special thanks to Dr. YK Yong for his valuable inputs and guidance.

My deepest gratitude is to my family. I have been amazingly fortunate to have such a wonderful family. Without the encouragement and motivation from my family this accomplishment would not have been possible. I would like to thank my many dear friends for listening to me, offering me advice and supporting me through the entire process.

.

Contents

Abstract	ii
Acknowledgments	iv
1 Introduction	1
1.1 Epoxy Systems	4
1.2 Inorganic Systems	10
1.3 Finite Element Based Approach	14
2 Model description and Analytical investigation	16
2.1 General	16
2.2 FE Modeling Of Steel Reinforcement	17
2.3 Element selection	20
2.3.1 SOLID 65	20
2.3.2 Link180	21
2.3.3 Solid45	21
2.4 Real Constants	22
2.5 Material Properties	24
2.5.1 Concrete	24
2.5.2 Steel Reinforcement and Steel Plates	29
2.5.3 Epoxy	31
2.5.4 Inorganic Polymer	32
2.6 Model Description	33

2.6.1	Beam Models I and II	34
2.6.2	Slab Model	42
3	Analysis Results And Discussion	48
3.1	Analysis	49
3.2	Results And Discussion	53
3.2.1	Effect Of Bond Slip On Load vs Deformation Response Of Beams	54
3.2.2	Beam Model I	59
3.2.3	Beam Model II	67
3.2.4	Slab Model	72
4	Conclusions and Recommendations	75
A	Appendix	81
A.1	Comparison Between Full Volume Model and Quarter Volume Model	81
A.2	Effect of Elastic Modulus of Filler Material on Stiffness	83
A.3	Effect of Shear Retention	87

List of Figures

1.1	Delaminated Concrete(Concreteanswers.org)	3
1.2	Kansas DOT's Custom Chuck(Klein)	7
1.3	Insertable Gasket Type Injection Probe(Klein)	8
1.4	Surface Mounted Type Injection Probe(Klein)	8
1.5	Chemical Structure Of Potassium Polysialate(Davidovits) . . .	11
2.1	Newton-Raphson Iterative Solution	17
2.2	Models For Reinforcement In Reinforced Concrete;(a) Dis- crete;(b) Embedded;(c) Smeared(Tavarez,2001)	18
2.3	Solid65-3D Reinforced Concrete Solid element in ANSYS . . .	20
2.4	Link180-3D Spar element in ANSYS	21
2.5	Solid45-3D Solid element in ANSYS	22
2.6	Typical uniaxial compressive and tensile stress-strain curve for concrete (Bangash 1989)	24
2.7	Simplified stress-strain model of concrete in compression . . .	27
2.8	3-D failure surface for concrete in ANSYS (Kachlakev 2000) .	28
2.9	Stress-strain curve for steel reinforcement	30
2.10	Stress-strain curve for Sealboss epoxy	31
2.11	Stress-strain curve for Inorganic Polymer	32
2.12	Input Parameters for Inorganic Polymer	33
2.13	ANSYS Model Of Quarter Beam	35

2.14 FE Mesh of the Concrete,Steel Plate,and Steel Support Beam for Model I	35
2.15 FE Mesh of the Concrete,Steel Plate,and Steel Support Beam for Model II	36
2.16 Steel Reinforcement In The FEM Model)	37
2.17 Full Scale Beam Dimensions tested by Klein (2013)	37
2.18 Photo of Notched Full-Scale Beams tested by Klein (2013) . .	38
2.19 Boundary Conditions For Planes Of Symmetry (Top View) . .	40
2.20 Boundary Conditions For Support	41
2.21 Boundary Conditions For Plate For Load Application	41
2.22 Volumes Created For ANSYS Quarter Slab Model	43
2.23 ANSYS FE mesh for the Quarter Slab Model	43
2.24 ANSYS Quarter FE model for Slab Model-Steel Reinforce- ment	44
2.25 Meshed Notch Elements Of The Slab Model	45
2.26 Boundary Conditions of The Slab Model	46
2.27 Support Conditions of The Slab Model	46
2.28 Point Loads At The Steel Plate	47
3.1 Input Data For The Non Linear Analysis In ANSYS	50
3.2 Solution Controls	51
3.3 Non Linear Solution Controls	51
3.4 Load vs Deformation Response From Experimental and Ana- lytical Results	54

3.5	COMBIN39 Element Properties In ANSYS	56
3.6	Bond-Slip Force Displacement Plot Input In ANSYS	57
3.7	Force Displacement Response Of Various Models	58
3.8	Cracked Pattern For Control I	61
3.9	Cracked Pattern For Notched Inorganic Beam I	61
3.10	Cracked Pattern For Epoxy Beam I	61
3.11	Stress Contour For Control I	62
3.12	Stress Contour For Inorganic Beam I	63
3.13	Stress Contour For Epoxy Beam I	63
3.14	Elastic Strain Variation of FEA Models	64
3.15	Load Displacement Plot	66
3.16	Stress Contours For Control II Model	67
3.17	Stress Contour For Notched Inorganic Beam II Model	68
3.18	Stress Contour For Notched Epoxy Beam II Model	68
3.19	Elastic Strain Variation of Beam Model II	69
3.20	Load Displacement Plot For Beam Model II	71
3.21	Load Displacement Plot Of Slab Model	73
A.1	Quarter Volume Model	81
A.2	Full Volume Model	82
A.3	Load Deformation Response from Quarter and Full Beams Models	82
A.4	Refined FE Mesh for Repaired Beam	83
A.5	Refined FE Mesh for Filler Region	84

A.6	Load Deformation Response, Organic Epoxy (yellow), Notched Beam (Green), Control Model (Blue), Inorganic Polymer (Orange)	84
A.7	Load Deformation Response from FE Models for Various Cases	86
A.8	Load Deformation Response for the Concrete Model	89
A.9	Load Deformation Response for Beam Repaired with Inorganic Polymer for Various Shear retention 0.1 and 0.3	90
A.10	Load Deformation Response for Beam Repaired with Organic Epoxy for Various Shear retention 0.1 and 0.3	91

List of Tables

1	Inorganic Polymer properties	13
2	Real constants	23
3	Dimensions for Concrete,Steel Plate,and Steel Support Volumes	34
4	Dimensions for Concrete,Steel Plate Volumes of The Slab Model	42
5	Dimensions of Notch In The Slab Model	44

1 Introduction

This thesis contains an investigation on inorganic aluminosilicate polymer for nondestructive rehabilitation of cracked concrete structural elements using a finite element based approach. The focus was to repair small width voids such as the delaminations and cracks developed due to restrained shrinkage and long-term distress in concrete bridge decks and other similar structural elements.

When fresh concrete is placed and compacted, the solids (cement and aggregate) settle. This natural settlement causes excess mix water and entrapped air to be displaced (called bleeding), and the lighter materials migrate toward the surface. If finishing operations start prematurely and close or seal the surface before bleeding is completed, air and or water are trapped under the dense surface mortar. As concrete hardens, subsurface voids develop where the water or air is trapped. These voids create weakened zones right below the surface and are also referred to as delaminations.

Restrained shrinkage cracking occurs when concrete is prevented from making volumetric changes by a source of restraint, either internal or external. The primary cause of drying shrinkage is the loss of adsorbed water, though the causes of the water loss for creep and drying shrinkage are radically different. For drying shrinkage, the driving force behind the water loss is the relative humidity. Restrained shrinkage induces tensile stresses in concrete

With the presence of cracks in concrete infrastructure for example bridge decks, water, sulfates, chlorides, and other potentially corrosive agents are able to permeate to the interior of the bridge deck. These agents cause further delamination and deterioration in the form of even larger cracks, spalling, potholes, and eventually a loss of cross section of the bridge deck or reinforcing steel, which ultimately leads to an unsafe bridge.

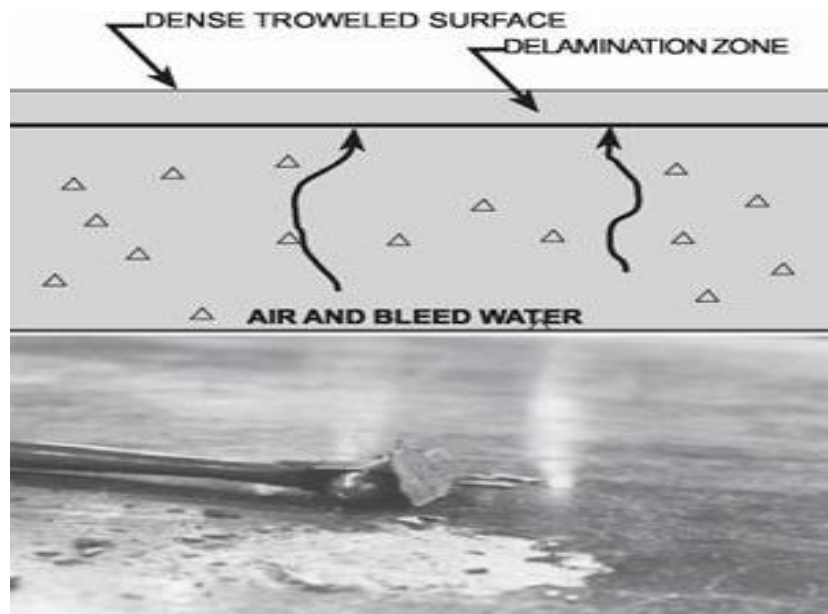


Figure 1.1: Delaminated Concrete(Concreteanswers.org)

The most popular method of repairing delaminated and the cracked concrete surface is to inject it with organic epoxy systems, if these cracks and delamination are left untreated, they will become larger causing major repairs to the affected areas, resulting in concrete removal and replacement and disruption to traffic.

1.1 Epoxy Systems

The first epoxies were designed both in America by Dr. S. O Greenlee and in Switzerland by Dr. Pierre Castan around 1935 (Epoxy Chemicals, Inc. 2013). The basic components of a 2- part epoxy have not changed since they were first formulated in the 1930s. The 2-part epoxy consists of a petroleum based resin and hardener or curative. The reaction is usually rapid and highly exothermic meaning excessive heat is produced when the resin and hardener are mixed in large quantities. The practice of repairing cracked concrete by epoxy injection had become popular by 1960 and the American Concrete Institute (ACI) published a method for its use (ACI Committee 403 1962).

In 1980 Kansas DOT investigated how long would the repair of bridge decks with epoxy actually last before the deck would have to be replaced (Stratton and Smith 1988). Four delaminated bridges were epoxy injected and compared to non injected bridges so that information on delamination repair durability and the frequency of repair could be collected. It was concluded that due to the organic nature of the resin and its susceptibility to breakdown by solvents and because the resin grows increasingly brittle over time, the injection repairs have to be done every 5 years on an average.

Also another study was conducted by Kansas DOT (1974) on how to choose an epoxy which would be suitable for the repairs. Early epoxy choices were arbitrary and subject to local availability. This initial epoxy also featured a higher viscosity, meaning pressures were greater on the original equipment.

Once an analytical survey had been completed, it was found that a lower viscosity epoxy was necessary to allow an effective repair solution. The Kansas DOT studied types of epoxy and gave an outline of the suitable feature set required for successful epoxy injection (Stratton and McCollom 1974, Connor 1979). Six epoxy systems were targeted to determine acceptable features. The following distributors were used: Kimmel Engineering Company (KR52-2 resin and KH-78 hardener), Sinmast of America, INC. (Sinmast Injection Resin), Adhesive Engineering Company (Concresive 1050-15), and the other three available from Sika Chemical Corporation (Colma Fix LV, Sikastix 37, and Sikadur Hi-Mod).

However, the epoxy available from Adhesive Engineering Company was not tested since the manufacturer limited usage to company trained and licensed technicians. In addition, early on it was discovered that the Kimmel Engineering Company supplied epoxy could be diluted in contact with moist conditions. Researchers had noted that water could be displaced from the delaminations during injection so the epoxy should be water-resistant.

The analytical research indicated that the maximum room temperature viscosity should be about 30 poise. The range of the tested epoxies was between 3 and 17 poise. The manufacturer low temperature curing requirements varied but the lowest was the epoxy manufactured by Sinmast at 33F and Sikadur Hi-Mod at 40F. All other systems minimum temperature was at about 60F. It was noted that the average low temperature in Kansas often

dipped below 60F at night. The remaining epoxies were tested for bond and durability against wetting and saline solutions by the use of flexural tests. These tests involved gluing concrete together and testing in flexure. In the durability tests, the specimens were soaked in water prior to repair and then kept in water during the epoxy curing. In all the dry bond cases the break location was located in the concrete except for the Sika Colma Fix LV which failed in the bond between the concrete and the epoxy. In the wetting tests, none of the epoxies survived 100% of the test. The Sikadur Hi Mod had the best performance with 75% concrete failure and the Sinmast followed with 66% concrete failure. The rest of the failure was in epoxy debonding. The Sinmast manufactured epoxy was recommended however because of its overall performance including low application temperature and viscosity.

A discussion on epoxy systems wouldn't be complete without discussing the way to transport the material to the delaminated zone. Initially a drill bit was used for reaching the delaminated zone. Fig 1.2 shows a modified drill bit which was developed by Kansas DOT, and is still commonly used.

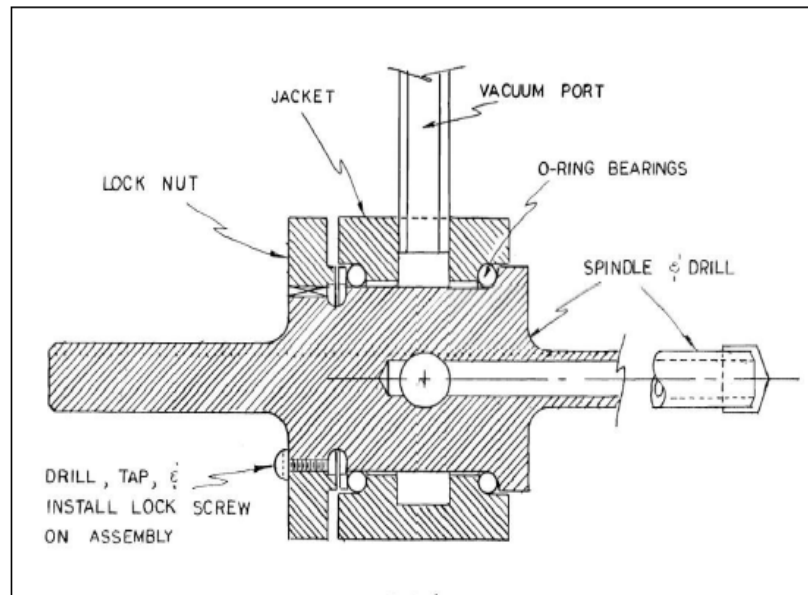


Figure 1.2: Kansas DOT's Custom Chuck(Klein)

Once a clear path free of blockage is made to the hollow plane, a connection had to be made between the epoxy injection equipment and the concrete deck. The first type of injection probe investigated was an insertable gasket type as shown in Fig 1.3.

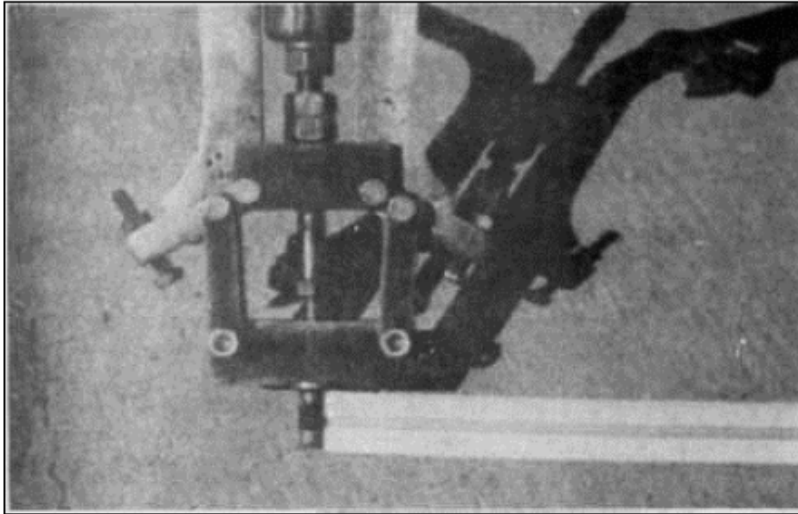


Figure 1.3: Insertable Gasket Type Injection Probe(Klein)

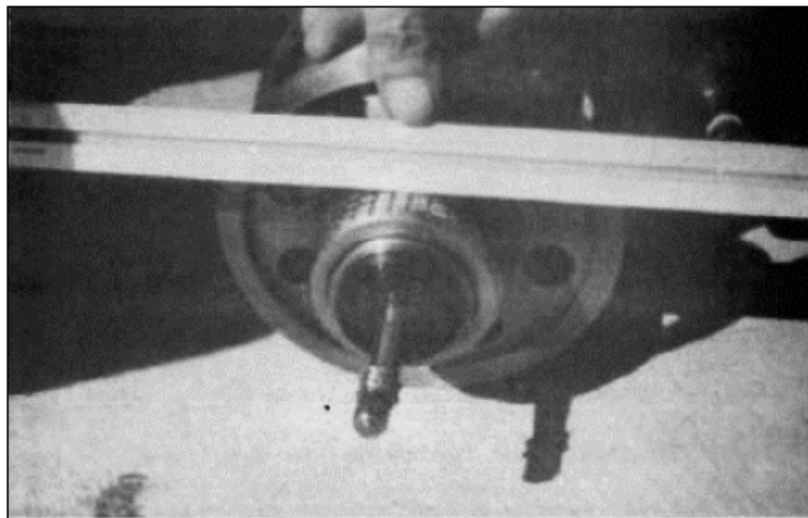


Figure 1.4: Surface Mounted Type Injection Probe(Klein)

The second type of injection probe still featured an insertable probe, but this

time, the gasket was surface mounted and held in place by the downward force of the technician who is operating the probe.

While the internal gasket type could withstand greater pressure and could remain in position without assistance during injection, it required a minimum depth of insertion to form an effective seal. In addition, the gasket took more time to replace since it involved removing the injection tip. The surface gasket type could resist leakage as long as the operator is using the equipment properly and a lower viscosity epoxy is used, however, if the surface was uneven, the seal could leak. The surface gasket type is prone to cause operator fatigue though it allowed for quick gasket replacements and quick injection set-up times.

Epoxy injection is so widely used because it can be used to seal off delaminations and cracks through the use of relatively inexpensive equipment and does not require a large labor force. Because of this, epoxy injection has become a cheaper repair alternative over jack-hammering out the affected area and replacing with fresh concrete. This allowed for less cost in man-hours and reduced lane closures since the areas repaired would not have to be shut down during the curing of the new concrete.

1.2 Inorganic Systems

In the 1970s a French scientist, Joseph Davidovits, developed a new class of inorganic plastics in response to several fire outbreaks in France (Davidovits 1979). The material that he found was a certain group of inorganic mineral compositions that shared similar hydrothermal conditions which control the synthesis of organic phenolic plastics, and of mineral feldspathoids and zeolites. Both syntheses required a high pH values, concentrated alkali, atmospheric pressure and thermoset at temperatures below 300F.

The result of this research was an entirely new family of materials that were given the name Geopolymer due of the geologic origin and how the materials share properties with other naturally occurring minerals such as feldspathoids, feldspars, and zeolites. These properties include thermal stability, smooth surfaces, hardness, weather resistant and high temperature resistant up to over 2000F. Unlike the naturally occurring minerals, the Geopolymers are polymers meaning they can be transformed, tooled, and molded. They are created in a similar manner to thermosetting organic resins and cement by poly condensation. The inorganic polymer can be formulated with or without the use of additional performance enhancing fillers or reinforcement. Applications of the material are found in automobile and aerospace industries, civil engineering and plastics/ceramics.

The terminology for the division of Geopolymers based on alumino-silicates is polysialate. Sialate is the acronym for silicon-oxo-aluminate of Na, K, Ca,

Li. The structure of the sialate is composed of SiO_4 and AlO_4 tetrahedrals linked by the shared oxygen. In the case of potassium alumino-silicates, the positive ion K^+ is present to balance the negative charge of the Al^{3+} in the IV-fold coordination. The chemical formula of the potassium polysialate is

$$\text{Kn}(-(\text{SiO}_2)_z - \text{AlO}_2)_n \cdot \text{H}_2\text{O}$$

where n is the degree of polycondensation and z is 1, 2, or 3. Polysialates are characterized as chain or ring polymers and in the case of the potassium alumino-silicate the resin hardens to a amorphous solid. The empirical formula of the potassium polysialate is $\text{Si}_{32}\text{O}_{99}\text{H}_{24}\text{K}_7\text{Al}$. Elemental composition, x-ray diffraction, and Si magic angle spinning nuclear magnetic resonance spectroscopy (Si MAS-NMR) have been used to create a representative structure of the cured inorganic material shown in Figure 1.5 (Davidovits 1991).

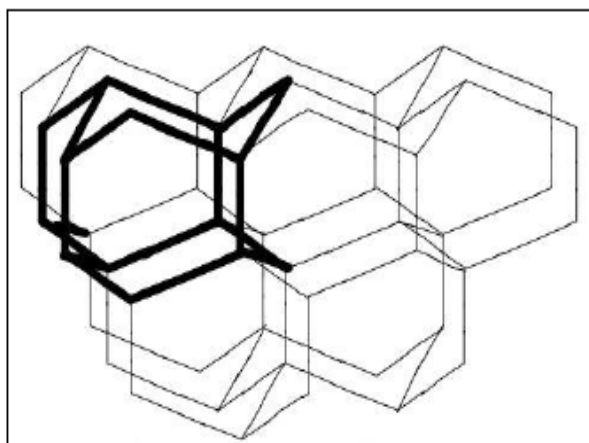


Figure 1.5: Chemical Structure Of Potassium Polysialate(Davidovits)

The properties of the inorganic polymer have been previously tested as a part of a long term research study done at Rutgers University under the guidance of Dr. P. N. Balaguru and in partnership with the Federal Aviation Administration and the Connecticut Department of Transportation. The results came largely from the dissertations of Andrew J. Foden(1999) and Ronald J. Garon (2000) and Matthew Klein (2013).

The properties of the inorganic polymer as shown in Table 1. were determined by conducting the following tests :

Tension: Tensile strength was determined based on ASTM C496 Standard Test Method for Splitting Tensile Strength of Cylindrical Concrete Specimens (ASTM C496 2011).

Compression, Strain, and Modulus of Elasticity: Compression strength was performed using ASTM D695 Standard Test Method for Compressive Properties of Rigid Plastics (ASTM D695 2010).

The dynamic modulus test was performed by measuring the compressive wave velocity in a sample. The dynamic shear modulus was found using the methods given by ASTM D4015 Standard Test Methods for Modulus and Damping of Soils by Resonant-Column Method (ASTM D4015 2007).

Surface Energy:The strain capacity and surface energy tests were performed using a technique by Deteresa et al, developed for determination of Kevler fiber properties (Deteresa et al 1984).

Flexural Strength: The tests for flexural strength, flexural modulus and fail-

ure strain were conducted in accordance with ASTM D790 Standard Test Methods for Flexural Properties of Unreinforced and Reinforced Plastics and Electrical Insulating Materials (ASTM D790 2010).

Table 1: Inorganic Polymer properties

Tensile stress	530 psi
Compression stress	5,665 psi
Tensile strain capacity	0.07%
Compressive strain capacity	0.49%
Modulus of Elasticity	1400000 psi
Surface Energy	0.000000994 Btu/in ²
Dynamic modulus of Elasticity	1570000 psi
Dynamic shear modulus	706 psi
Flexural strength	1170000 psi
Flexural modulus	1360000 psi
Flexural strain	0.86%
Poissons's ration	0.244

Inorganic polymer can be considered as an alternative to epoxy due its compatibility with concrete. The material property is shown in Table 1., were used in the finite element model as explained in the next section.

1.3 Finite Element Based Approach

Typically, the behavior of reinforced concrete beams is studied by full-scale experimental investigations. Response quantities such as deflections and internal stress or strain distributions within the beam are compared to theoretical calculations. Finite element analysis can also be used to model the behavior numerically to confirm these calculations, as well as to provide a valuable supplement to the laboratory investigations, particularly in parametric studies. Finite element analysis, as used in structural engineering, determines the overall behavior of a structure by dividing it into a number of simple elements, each of which has well-defined mechanical and physical properties.

Modeling the complex behavior of reinforced concrete, which is both non homogeneous and anisotropic, is a difficult challenge in the finite element analysis of civil engineering structures. Most early finite element models of reinforced concrete included the effects of cracking based on a pre-defined crack pattern (Ngo and Scordelis 1967, Nilson 1968). With this approach, changes in the topology of the models were required as the load increased; therefore, the ease and speed of the analysis were limited. A smeared cracking approach was introduced using isoparametric formulations to represent the cracked concrete as an orthotropic material (Rashid 1968). In the smeared cracking approach, cracking of the concrete occurs when the principal tensile stress exceeds the ultimate tensile strength. The elastic modulus of the material

is then assumed to be zero in the direction parallel to the principal tensile stress direction(Suidan and Schnobrich 1973).

In recent years, however, the use of finite element analysis has increased due to progressing knowledge and capabilities of computer software and hardware. It has now become the method of choice to analyze concrete structural components. The use of computer software to model these elements is much faster, and extremely cost-effective. Data obtained from a finite element analysis package is not useful unless the necessary steps are taken to understand what is happening within the model that is created using the software. Also, executing the necessary checks along the way is key to make sure that what is being output by the computer software is valid. By understanding the use of finite element packages, more efficient and better analyses can be made to fully understand the response of individual structural components and their contribution to a structure as a whole

This thesis is a study of reinforced concrete beams and slabs repaired with inorganic polymer and epoxy using finite element analysis to understand the response of repaired reinforced concrete structures when loaded till failure.

2 Model description and Analytical investigation

2.1 General

As mentioned, the behavior of reinforced concrete beams is usually studied by full-scale experimental investigations, in this thesis we study the behavior of reinforced concrete beams using finite element analysis. The experimental work done by Klien (Klein 2013) on experimental investigation of reinforced concrete beams repaired with inorganic polymer and epoxy is used as a reference and comparisons are made between the finite element approach and experimental investigations. The load displacement response from the finite element analysis was compared to the experimental.

A literature review was conducted on which FEA software to be used to model the behavior of reinforced concrete. ANSYS 14.5 was selected because of its ability to model concrete elements. In this study, the reinforced concrete model was loaded until failure. ANSYS employs the "Newton-Raphson" approach to solve nonlinear problems. In this approach, the load is subdivided into a series of load increments. The load increments can be applied over several load steps. Figure 2.1 illustrates the use of Newton-Raphson equilibrium iterations in a single DOF nonlinear analysis.

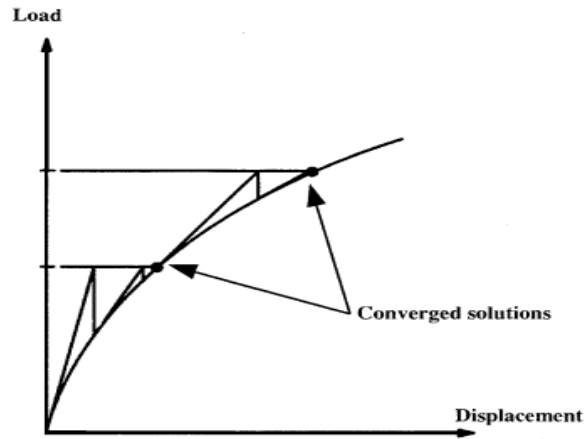


Figure 2.1: Newton-Raphson Iterative Solution

Before each solution, the Newton-Raphson method evaluates the out-of-balance load vector, which is the difference between the restoring forces (the loads corresponding to the element stresses) and the applied loads. The program then performs a linear solution, using the out-of-balance loads, and checks for convergence. If convergence criteria are not satisfied, the out-of-balance load vector is re-evaluated, the stiffness matrix is updated, and a new solution is obtained. This iterative procedure continues until the problem converges.

2.2 FE Modeling Of Steel Reinforcement

Tavarez (2001) discusses three techniques that exist to model steel reinforcement in finite element models for reinforced concrete (Figure 2.2): the dis-

crete model, the embedded model, and the smeared model. The reinforcement in the discrete model (Figure 2.2a) uses bar or beam elements that are connected to concrete mesh nodes. Therefore, the concrete and the reinforcement mesh share the same nodes and concrete occupies the same regions occupied by the reinforcement. A drawback to this model is that the concrete mesh is restricted by the location of the reinforcement and the volume of the steel reinforcement is not deducted from the concrete volume.

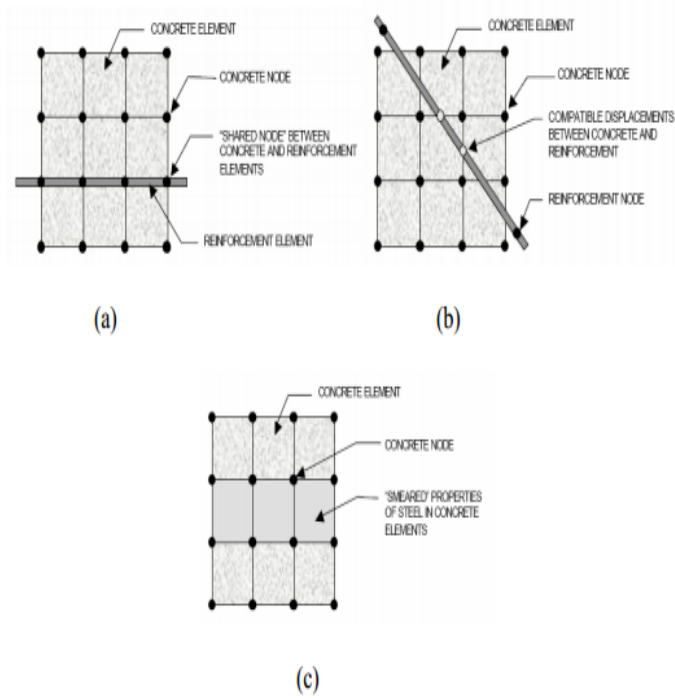


Figure 2.2: Models For Reinforcement In Reinforced Concrete;(a) Discrete;(b) Embedded;(c) Smeared(Tavarez,2001)

The embedded model (Figure 2.2b) overcomes the concrete mesh restrictions because the stiffness of the reinforcing steel is evaluated separately from the concrete elements. The model is built in a way that keeps reinforcing steel displacements compatible with the surrounding concrete elements. When reinforcement is complex, this model is very advantageous. However, this model increases the number of nodes and degrees of freedom in the model, therefore, increasing the run time and computational cost.

The smeared model (Figure 2.2c) assumes that reinforcement is uniformly spread throughout the concrete elements in a defined region of the FE mesh. This approach is used for large-scale models where the reinforcement does not significantly contribute to the overall response of the structure. Fanning (2001) and Wolanski (2004) modeled the response of the reinforcement using the discrete model and the smeared model for reinforced concrete beams. It was found that the best modeling strategy was to use the discrete model when modeling reinforcement.

2.3 Element selection

2.3.1 SOLID 65

An eight-node solid element, SOLID65, was used to model the concrete and the inorganic polymer. SOLID65 is used for the three-dimensional modeling of solids with or without reinforcing bars (rebars). The solid is capable of cracking in tension and crushing in compression. In concrete applications, for example, the solid capability of the element may be used to model the concrete while the rebar capability is available for modeling reinforcement behavior. The element is defined by eight nodes having three degrees of freedom at each node: translations in the nodal x, y, and z directions. Up to three different rebar specifications may be defined. The geometry and node locations for this element type are shown in figure 2.3 .

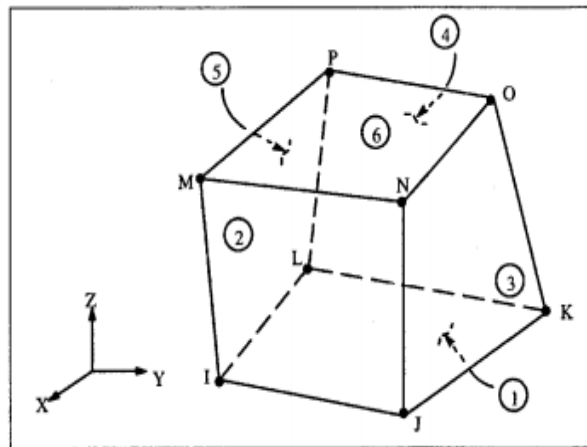


Figure 2.3: Solid65-3D Reinforced Concrete Solid element in ANSYS

2.3.2 Link180

A Link180 element was used to model the steel reinforcement. The three-dimensional spar element is a uniaxial tension-compression element with three degrees of freedom at each node: translations in the nodal x, y, and z directions. As in a pin-jointed structure, no bending of the element is considered. Plasticity, creep, swelling, stress stiffening, and large deflection capabilities are included. The geometry and node locations for this element is shown in figure 2.4 .

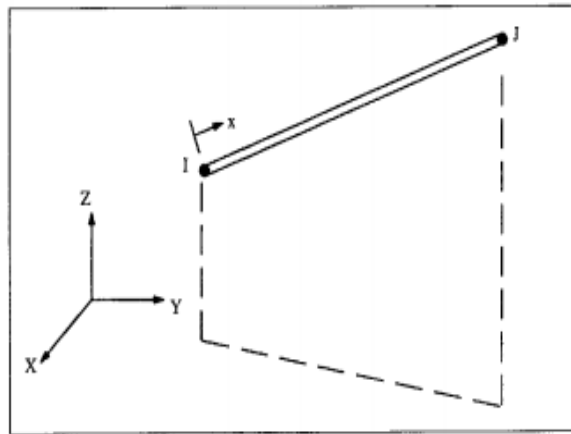


Figure 2.4: Link180-3D Spar element in ANSYS

2.3.3 Solid45

An eight-node solid element, Solid45, was used for the steel plates at the supports and at the loading location in the models. Solid45 is used for the

three-dimensional modeling of solid structures. The element is defined by eight nodes having three degrees of freedom at each node: translations in the nodal x, y, and z directions. The element has plasticity, creep, stress stiffening, large deflection, and large strain capabilities. The geometry and node locations for this element type are shown in figure 2.5 .

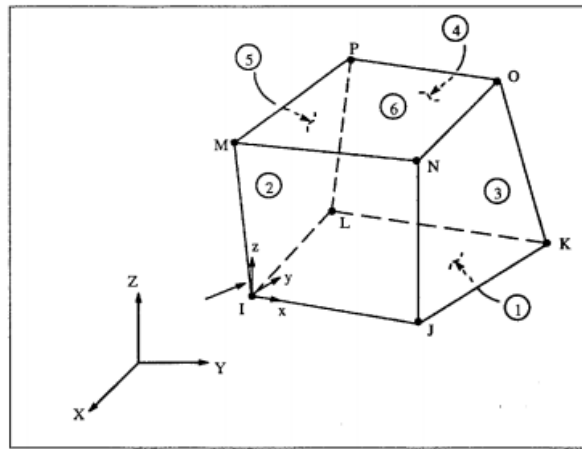


Figure 2.5: Solid45-3D Solid element in ANSYS

2.4 Real Constants

The real constants for concrete element and steel element are shown in Table 2. Note that individual elements contain different real constants. No real constant set exists for the element Solid45 .

Real Constant Set 1 was used for the element Solid65 element. It requires real constants for rebar assuming a smeared model. Values can be entered for Material Number, Volume Ratio, and Orientation Angles. The material

Table 2: Real constants

Real Constant Set	Element Type	Constants			
1	Solid 65		rebar 1	rebar 2	rebar 3
		Material number	0	0	0
		Volume ratio	0	0	0
		Orientation angle	0	0	0
		Orientation angle	0	0	0
2	Link 180	Cross-sectional area	0.39		
3	Link 180	Cross sectional area	0.15		

number refers to the type of material for the reinforcement. The volume ratio refers to the ratio of steel to concrete in the element. The orientation angles refer to the orientation of the reinforcement in the smeared model. ANSYS allows the user to enter three rebar materials in the concrete. Each material corresponds to x, y, and z directions in the element. The reinforcement has uniaxial stiffness and the directional orientation is defined by the user. In the present study the beam is modeled using discrete reinforcement. Therefore, a value of zero was entered for all real constants which turned the smeared reinforcement capability of the Solid65 element off.

Real Constant Sets 2 and 3 are defined for the Link 180 element. Values for cross-sectional area were entered. Cross-sectional areas in sets 2 and 3 refer to the reinforcement of 3-#6 bars Cross-sectional areas in set 3 refer to the #3 stirrups.

2.5 Material Properties

2.5.1 Concrete

To develop a model for the behavior of concrete is a challenging task. Concrete is quasi-brittle material and has different behavior in compression and tension. The tensile strength of concrete is typically 8-15% of the compressive strength(Shah,et al. 1995). Figure 2.6 shows a typical stress-strain curve for normal weight concrete(Bangash 1989).

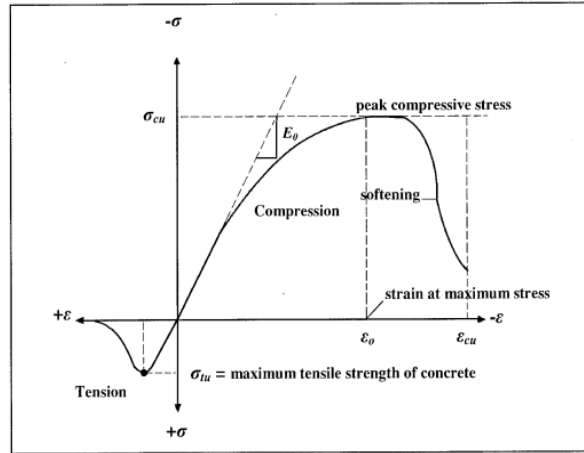


Figure 2.6: Typical uniaxial compressive and tensile stress-strain curve for concrete (Bangash 1989)

In compression, the stress-strain curve for concrete is linearly elastic up to about 30% of the maximum compressive strength. Above this point, the stress increases gradually up to the maximum compressive strength. After it reaches the maximum compressive strength σ_{cu} , the curve descends into a

softening region, and eventually crushing failure occurs at an ultimate strain ϵ_{cu} . In tension, the stress-strain curve for concrete is approximately linearly elastic up to the maximum tensile strength. After this point, the concrete cracks and the strength decreases gradually to zero (Bangash 1989).

For concrete, ANSYS requires the following input data for material properties.

Elastic modulus (E_c).

Ultimate uniaxial compressive strength(f'_c).

Ultimate uniaxial tensile strength(modulus of rupture, f_r).

Poisson's ratio (ν).

Shear transfer coefficient(β_t).

Compressive uniaxial stress-strain relationship for concrete.

The elastic modulus of concrete is taken from the experimental investigation conducted by (Klein 2013). From elastic modulus , the ultimate concrete compressive and tensile strength were calculated by Equations 2.4.1 and 2.4.2 (ACI 318,1999).

$$f'_c = \left(\frac{E_c}{57000}\right)^2 \quad (2.5.1)$$

$$f_r = 7.5\sqrt{f'_c} \quad (2.5.2)$$

where E_c, f'_c and f_r are in psi.

Poisson's ratio was taken as 0.18 in the FE model. The shear transfer coefficient, β_t , represents conditions of the crack face. The value of β_t ranges from 0.0 to 1.0, with 0.0 representing a smooth crack (complete loss of shear)

and 1.0 representing a rough crack(no loss of shear). The value of β_t used in many studies of reinforced concrete structures, however, varied between 0.05 and 0.25(Bangash 1989,Husye.et al 1994,Kachlakev and Miller 2000). A value of 0.3 was selected in this study keeping solution convergence in mind.

Uniaxial Stress-Strain Relationship For Concrete The ANSYS program requires the uniaxial stress-strain relationship for concrete in compression. Numerical expressions(Desayi and krishnan 1964) from equations 2.4.3 and 2.4.4,were used along with equation 2.4.5(Gere and Timoshenko 1997) to construct the uniaxial compressive stress-strain curve for concrete in this study.

$$f = \frac{E_c \epsilon}{1 + \left(\frac{\epsilon}{\epsilon_o}\right)^2} \quad (2.5.3)$$

$$\epsilon_o = \frac{2f'_c}{E_c} \quad (2.5.4)$$

$$E_c = \frac{f}{\epsilon} \quad (2.5.5)$$

where:

f=stress at any strain ϵ ,psi

ϵ = strain at stress f

ϵ_o = strain at the ultimate compressive strength f'_c

Figure 2.7 shows the simplified compressive uniaxial stress-strain relationship

that was used in this study. In this study, an assumption was made of perfectly plastic behavior after the last data point.

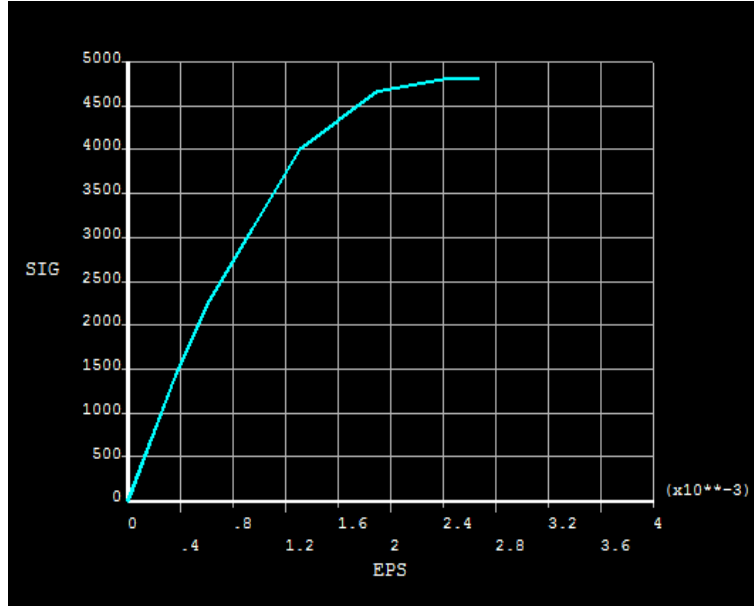


Figure 2.7: Simplified stress-strain model of concrete in compression

Failure Criteria Of Concrete The developed model is capable of predicting failure of concrete materials for both cracking and crushing failure modes. The two input strength parameters needed to define the failure surface for the concrete are the ultimate tensile and compressive strengths . Consequently, a criterion for failure of the concrete due to a multiaxial stress state can be calculated from these input parameters(William and Warnke 1975).

A three-dimension failure surface for concrete is shown in Figure 2.8 . The

most significant nonzero principal stresses are in the x and y directions, represented by σ_{xp} and σ_{yp} , respectively. Three failure surfaces are shown as projections on the σ_{xp} - σ_{yp} plane. The mode of failure is a function of the sign σ_{zp} (principal stress in the z direction). For example, if σ_{xp} and σ_{yp} are both negative (compressive) and σ_{zp} is slightly positive (tensile), cracking would be predicted in a direction perpendicular to σ_{zp} . However, if σ_{zp} is zero or slightly negative, the material is assumed to crush (ANSYS).

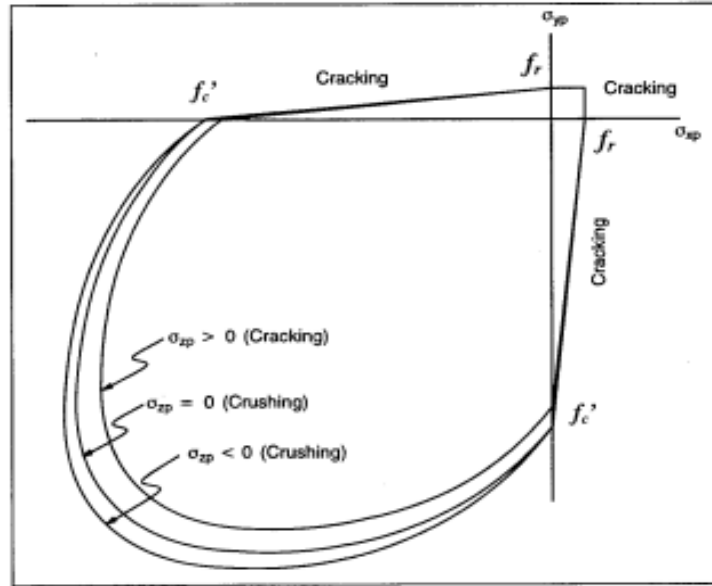


Figure 2.8: 3-D failure surface for concrete in ANSYS (Kachlakev 2000)

In a concrete element, cracking occurs when the principal tensile stress in any direction lies outside the failure surface. After cracking, the elastic modulus of the concrete element is set to zero in the direction parallel to the principal tensile stress direction. Crushing occurs when all principal stresses are com-

pressive and lie outside the failure surface;subsequently, the elastic modulus is set to zero in all directions,and the element effectively disappears(ANSYS).

In this study, it was found that if the crushing capability of the concrete is turned on, the finite element beam models fail prematurely. Crushing of the concrete started to develop in elements located directly under the loads. Subsequently, adjacent concrete elements crushed within several load steps as well, significantly reducing the local stiffness.

A pure "compression" failure of concrete is unlikely. In a compression test, the specimen is subjected to a uniaxial compressive load. Secondary tensile strains induced by poisson's effect occur perpendicular to the load. Because concrete is relatively weak in tension, these stresses actually cause cracking and the eventual failure (Mindess and Young 1981;Shah,et al.1995,Kachlakev and Miller 2000). In this study, the crushing capability was turned off and cracking of the concrete controlled the failure of the finite element models.

2.5.2 Steel Reinforcement and Steel Plates

Steel reinforcement in the experimental beams was constructed with typical Grade 60 steel reinforcing bars (Klein 2013). The elastic modulus and yield stress for the steel reinforcement used in the FE were the same material properties used in the experimental investigation. The steel for the finite element models was assumed to be an elastic-perfectly plastic material and identical in tension and compression. A Poisson's ratio of 0.3 was used for

the steel reinforcement in the study (Gere and Timoshenko 1997). Figure 2.9 shows the stress-strain relationship of steel reinforcement used in the FE analysis in this study. Material properties for the steel reinforcement for all the models were as follows :

Elastic modulus, $E_s = 2.9\text{E}+07$ psi

Yield stress, $f_y = 60,000$ psi

Poisson's ratio, $\nu = 0.3$

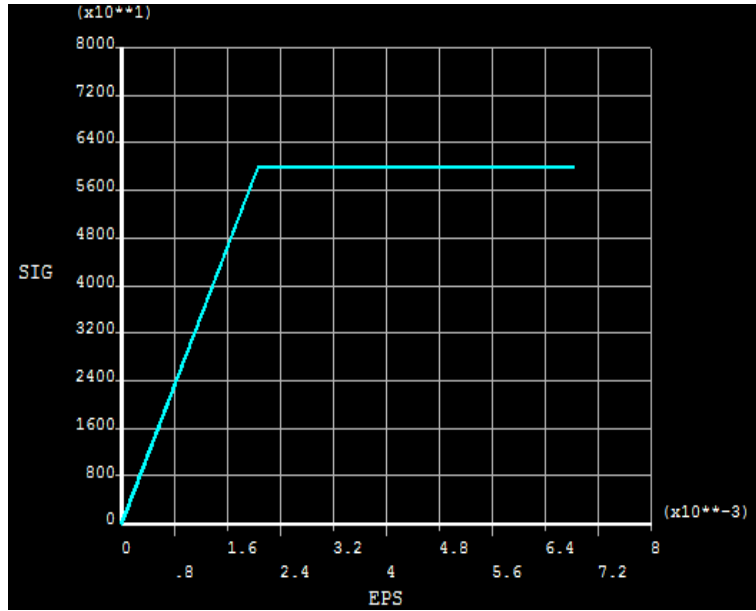


Figure 2.9: Stress-strain curve for steel reinforcement

Steel plates were added at support locations and at load application location in the finite element models (as in the actual beams) to provide a uniform stress distribution over the support areas. An elastic modulus equal to $2.9\text{E}+07$ psi and Poisson's ratio of 0.3 were used for the steel plates. The

steel plates were assumed to be linear elastic materials.

2.5.3 Epoxy

The epoxy used in the experimental beams was Sealboss 4040 resin which is commercially available (Klein 2013). Epoxy properties such as , elastic modulus and stress-strain behavior used in the FEA study were taken from literature available from Sealboss product data. The modulus of elasticity and Poisson's ratio of the Sealboss epoxy were $1.842\text{E}+05$ psi and 0.3 respectively . Figure 2.10 shows the stress-strain relationship of epoxy used in the nonlinear FEA .

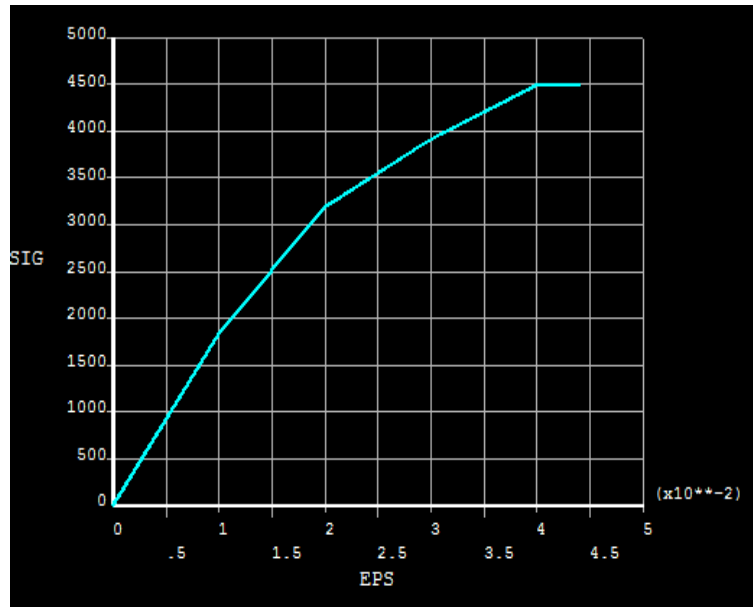


Figure 2.10: Stress-strain curve for Sealboss epoxy

2.5.4 Inorganic Polymer

The mechanical properties of the inorganic polymer used in this study such as tensile strength and modulus of elasticity were obtained from experimental analysis conducted on the inorganic polymers by Foden (1999), Garon(2000) and Klein(2013). These values were give in Table 1 in chapter 1. Figure 2.11 shows the stress-strain relationship of the inorganic polymer for all the FE models.

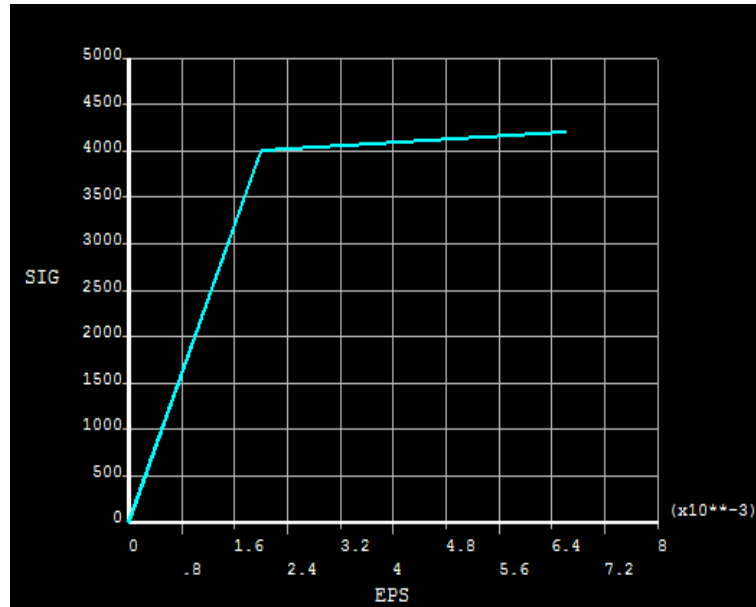


Figure 2.11: Stress-strain curve for Inorganic Polymer

The inorganic polymer was modeled using solid 65 elements in the FE models similar to concrete, as it shares a lot of similarity with concrete. Fig 2.12 shows the input parameters used to define the inorganic polymer behavior.

	T1
Temperature	0
Open Shear Transfer Coef	0.3
Closed Shear Transfer Coef	1
Uniaxial Cracking Stress	530
Uniaxial Crushing Stress	-1
Biaxial Crushing Stress	0
Hydrostatic Pressure	0
Hydro Biax Crush Stress	0
Hydro Uniax Crush Stress	0
Tensile Crack Factor	0

Figure 2.12: Input Parameters for Inorganic Polymer

The open shear transfer coefficient was taken 0.3 similar to concrete and the tensile strength of material was taken from Table 1. The crushing stress was turned off similar to the concrete model.

2.6 Model Description

To compare the behavior of beams and slabs repaired with inorganic polymer and with epoxy, various FE models were developed in this study. The response was also compared to the unrepaired concrete model. Initially a beam model similar to the experimental beam model tested by klein(2013) was considered and also a comparison was made between analytical and ex-

perimental investigations in the future chapters. The thickness of the notch to be repaired with polymers was varied to see the effect of the size of the void on the behavior of structure. Lastly a slab model was modeled to see the behavior of the slab repaired in multiple locations with the polymer. The descriptions of each model is as follows.

2.6.1 Beam Models I and II

The dimensions of the full-size beams were 96 in x 8 in x 8 in. The beam, plates, and supports were modeled as volumes. Since a quarter of the beam is being modeled, the model is 48 in. long, with a cross-section of 4 in. x 8 in. The dimensions for the concrete volume are shown in Table 3. Due to symmetry, only one loading plate and one support plate were needed. The support was modeled using 2 in. x 4 in. x 1 in. steel plate, and at load point was 4 in. x 4 in. x 1 in. The dimensions for the plates and supports are shown in Table 3. The plates, supports, and beam geometry are shown in Figure 2.13. The FE mesh for the beam model is shown in Figure 2.14.

Table 3: Dimensions for Concrete,Steel Plate,and Steel Support Volumes

ANSYS	Concrete		Steel Plate		Steel Support	
X1,X2 X-coordinates	0	48	30	34	0	2
Y1,Y2 Y-coordinates	0	8	8	9	0	-1
Z1,Z2 Z-coordinates	0	4	0	4	0	4

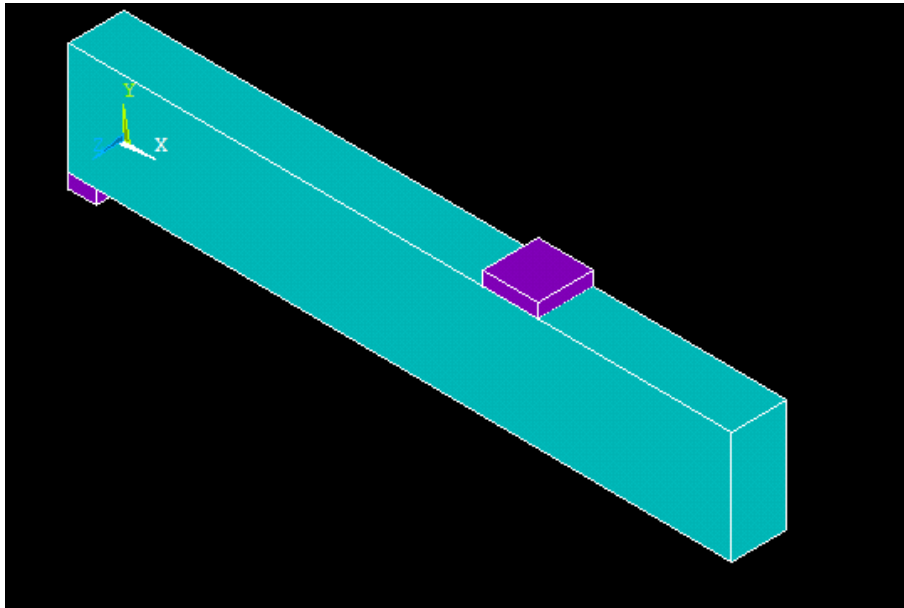


Figure 2.13: ANSYS Model Of Quarter Beam

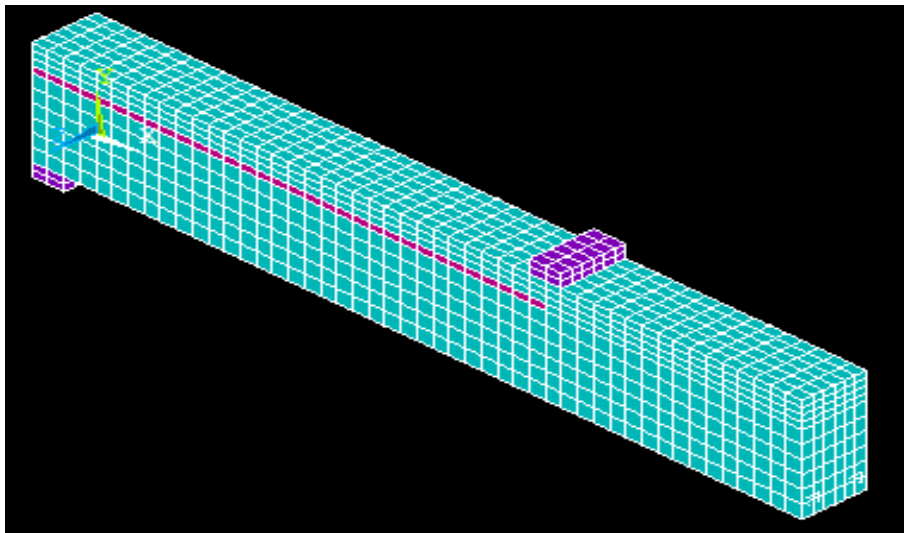


Figure 2.14: FE Mesh of the Concrete, Steel Plate, and Steel Support Beam for Model I

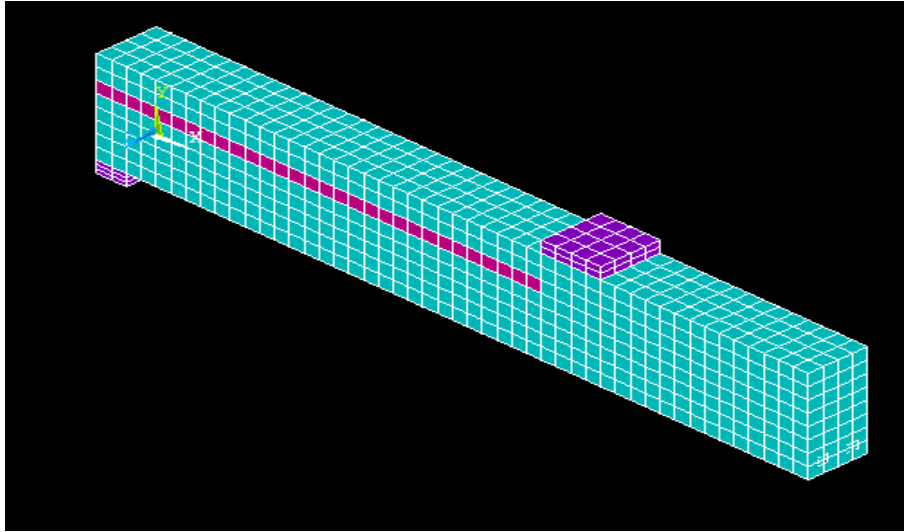


Figure 2.15: FE Mesh of the Concrete, Steel Plate, and Steel Support Beam for Model II

Fig 2.14 shows a notch which is two third of the length of the beam and 4 inch wide. The thickness of notch was taken as 0.5 inch in model beam I. Figure 2.15 shows beam model II which is similar to beam model I except the notch is 1 inch thick. Three FE models were created to analyze the effect of the filling material on the beam response to applied loads. One model has concrete as filler material while the other two models use inorganic polymer and epoxy as filler materials. ANSYS Link 180 elements were used to create the flexural and shear reinforcement for the beam, Fig 2.16 shows the reinforcement in the FE model. The dimensions of the beam were taken similar to those in Klein's study (2013). The dimensions of the beam tested by Klein (2013) is shown in Figure 2.16., figure 2.17 shows a photo of 5 beams

tested by klein(2013) with different filler materials.

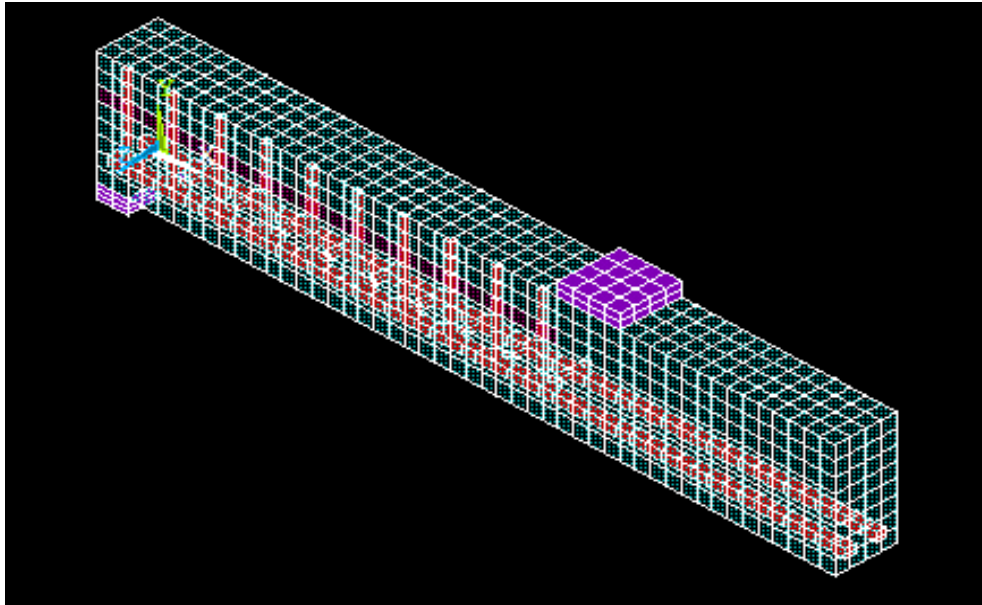


Figure 2.16: Steel Reinforcement In The FEM Model)

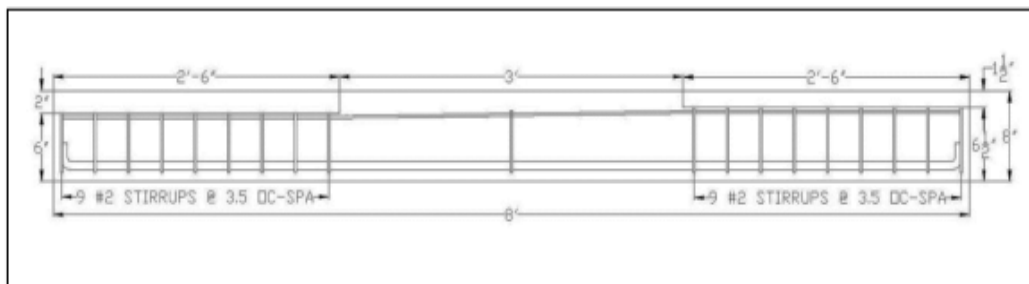


Figure 2.17: Full Scale Beam Dimensions tested by Klein (2013)



Figure 2.18: Photo of Notched Full-Scale Beams tested by Klein (2013)

To obtain good results from the Solid65 element, the use of a rectangular mesh is recommended. Therefore, the mesh was set up such that square or rectangular elements were used (Figure 2.14). The volume sweep command was used to mesh the steel plate and support. This properly sets the width and length of elements in the plates to be consistent with the elements and nodes in the concrete portions of the model. The overall mesh of the concrete, plate, and support volumes is shown in Figure 2.14. The necessary element divisions are noted. The meshing of the reinforcement is a special case compared to the volumes. No mesh of the reinforcement is needed because individual elements were created in the modeling through the nodes created by the mesh of the concrete volume.

The command "merge items" merges separate entities that have the same location. These items will then be merged into single entities. Caution must be taken when merging entities in a model that has already been meshed because the order in which merging occurs is significant. Merging keypoints before nodes can result in some of the nodes becoming orphaned; that is, the nodes lose their association with the solid model. The orphaned nodes can cause certain operations (such as boundary condition transfers, surface load transfers, and so on) to fail. Care must be taken to always merge in the order that the entities appear. All precautions were taken to ensure that everything was merged in the proper order. Also, the lowest number was retained during merging.

Displacement boundary conditions are needed to constrain the model to get a unique solution. To ensure that the model acts the same way as the experimental beam, boundary conditions need to be applied at points of symmetry, and where the supports and loads exist. The symmetry boundary conditions were set first. The model being used is symmetric about two planes. The boundary conditions for both planes of symmetry are shown in Figure 2.19.

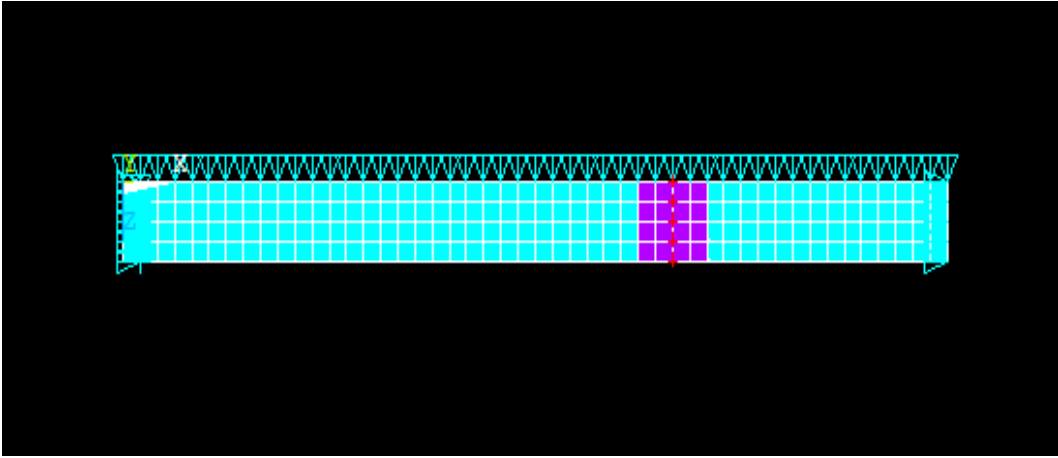


Figure 2.19: Boundary Conditions For Planes Of Symmetry (Top View)

Nodes defining a vertical plane through the beam cross-section centroid defines a plane of symmetry. To model the symmetry, nodes on this plane must be constrained in the perpendicular direction. These nodes, therefore, have a degree of freedom constraint $UX = 0$. Second, all nodes selected at $Z = 0$ define another plane of symmetry. These nodes were given the constraint $UZ = 0$. A single line of nodes on the plate were given constraint in the UX , UY , and UZ directions, applied as constant values of 0 at the support. By doing this, the beam will be allowed to rotate at the support. The support condition is shown in Figure 2.20.

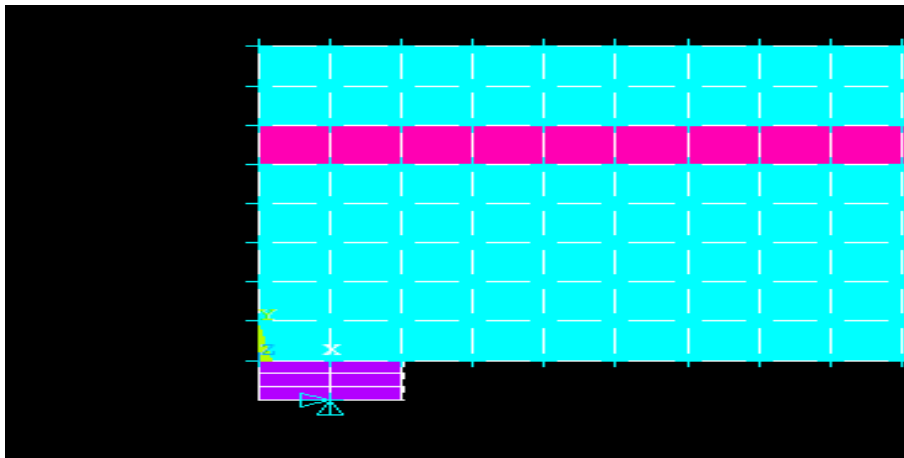


Figure 2.20: Boundary Conditions For Support

The force, P , applied at the steel plate is applied across the entire center line of the plate. The force applied at each node on the plate is one tenth of the actual force applied. Figure 2.21 illustrates the plate and applied loading

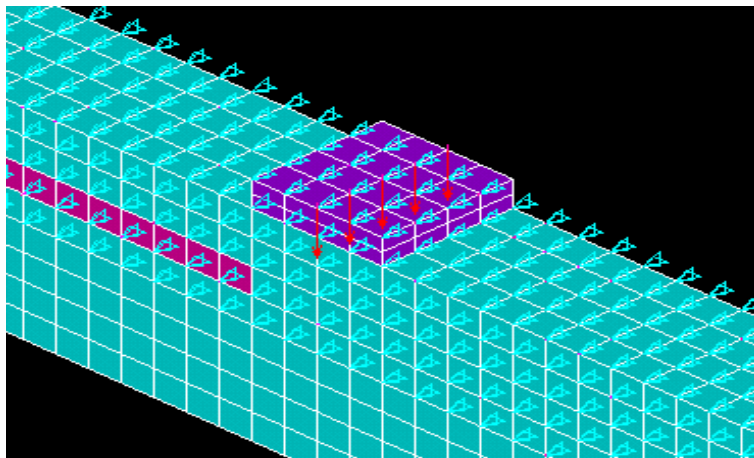


Figure 2.21: Boundary Conditions For Plate For Load Application

2.6.2 Slab Model

The dimensions of the slab model considered in this study were 144 in x 72 in x 8 in. The slab, and plates were modeled as volumes. To reduce the size of the model and computation time, a quarter of the slab was modeled by taking advantage of symmetry of loads and geometry. The quarter model was 72 in. long, with a width of 36 in and a height of 8 in. The dimensions for the concrete volume are shown in Table 4. Due to symmetry, only one loading plate is needed and the location of the loading plate is shown in Figure 2.22 . The steel plate at the load point is 4 in. x 4 in. x 1 in. The dimensions for the plate and the slab are shown in Table 4. The combined volumes of the plate and slab are shown in Figure 2.22. The FE mesh for the quarter slab model is shown in Figure 2.23.

Table 4: Dimensions for Concrete,Steel Plate Volumes of The Slab Model

ANSYS	Concrete		Steel Plate	
X1,X2 X-coordinates	0	72	68	72
Y1,Y2 Y-coordinates	0	8	8	9
Z1,Z2 Z-coordinates	0	36	32	36

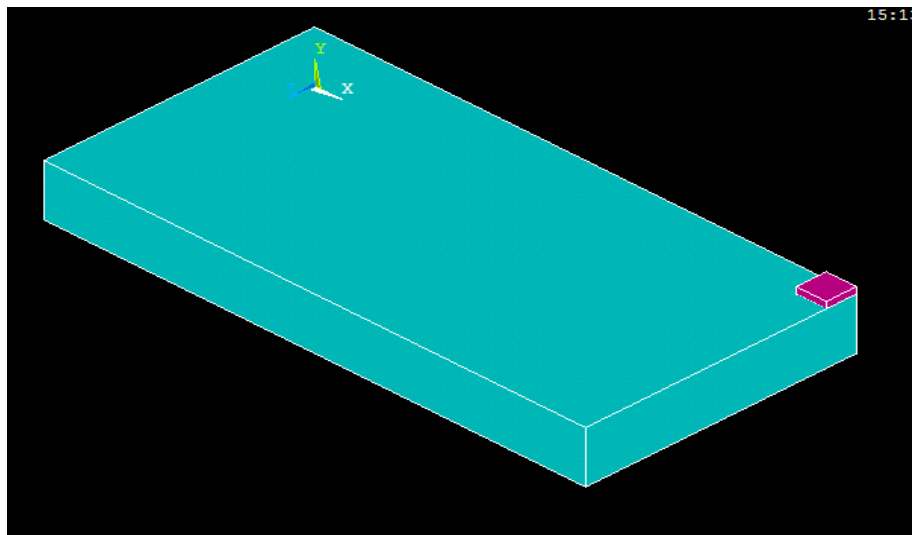


Figure 2.22: Volumes Created For ANSYS Quarter Slab Model

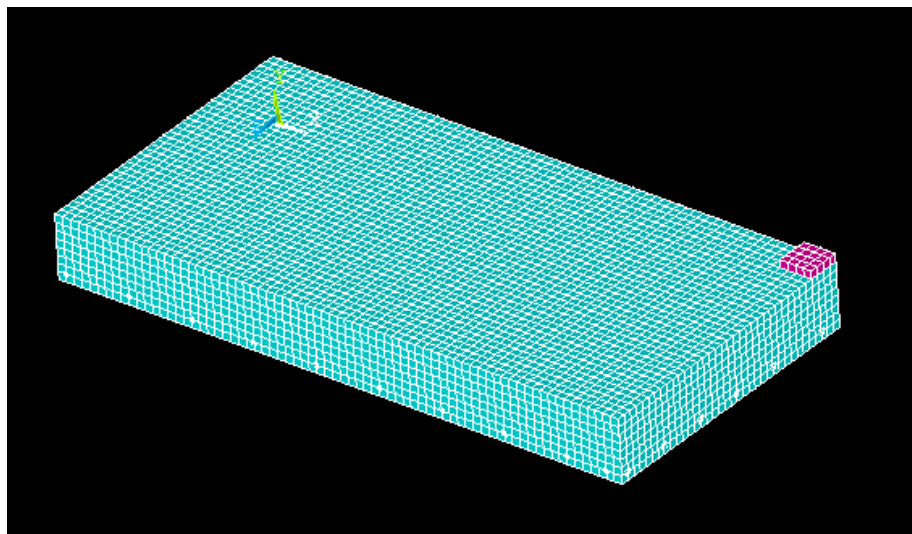


Figure 2.23: ANSYS FE mesh for the Quarter Slab Model

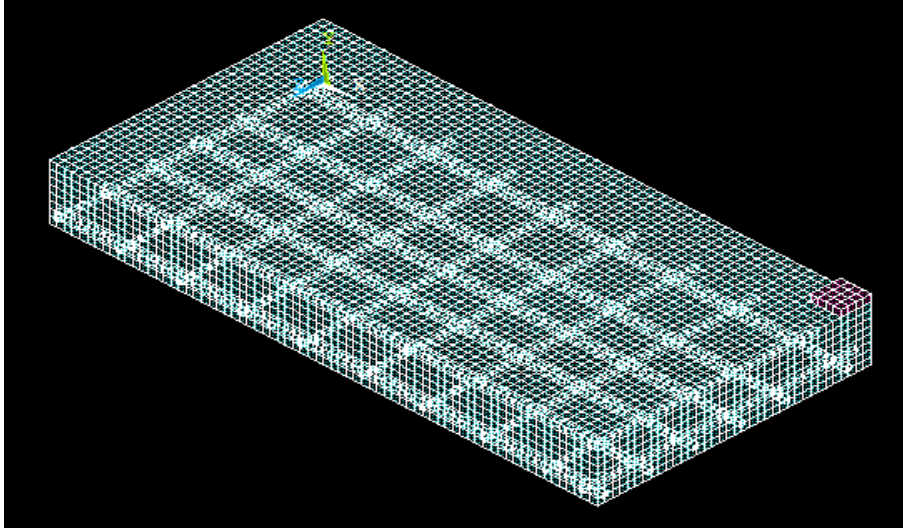


Figure 2.24: ANSYS Quarter FE model for Slab Model-Steel Reinforcement

Link 180 elements were used to create the flexural reinforcement in both the longitudinal and transverse directions. Fig 2.24 shows the reinforcement in the FE model. Four quarter slab models were created with three different filler materials in the notch and a unrepaired slab model:(1) concrete, (2) epoxy , (3) inorganic polymer and (4) Void . The slab model has multiple notches of 1 inch in thickness. The location of the notches is shown in Figure 2.25 and the notch locations and their dimensions are shown in Table 5.

Table 5: Dimensions of Notch In The Slab Model

ANSYS	Notch 1		Notch 2		Notch 3	
X1,X2 X-coordinates	11	21	31	41	51	61
Y1,Y2 Y-coordinates	5	6	5	6	5	6
Z1,Z2 Z-coordinates	6	26	6	26	6	26

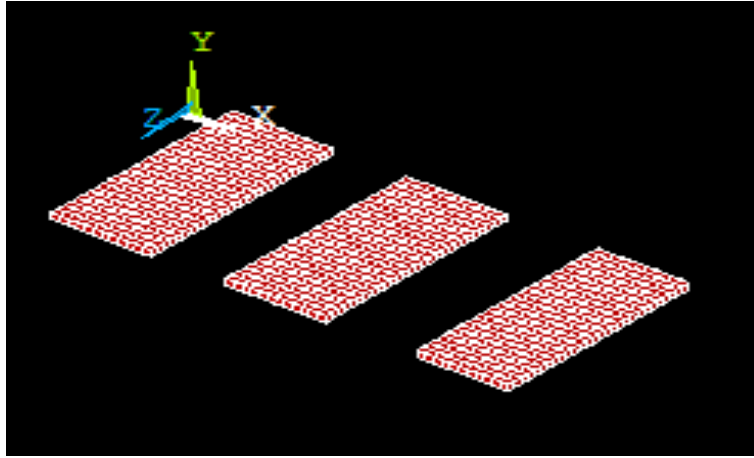


Figure 2.25: Meshed Notch Elements Of The Slab Model

Displacement boundary conditions are needed to constrain the model to get a unique solution. The symmetry boundary conditions were set first. Nodes defining a vertical plane through the slab cross-section centroid defines a plane of symmetry. To model the symmetry, nodes on this plane must be constrained in the perpendicular direction. These nodes, therefore, have a degree of freedom constraint $UX = 0$. Second, all nodes selected at $Z = 0$ define another plane of symmetry. These nodes were given the constraint $UZ = 0$. The support conditions were set along a line at the corner of the slab in both X- direction and Z-direction, constraints were given to the selected nodes in the UX, UY, and UZ directions, applied as constant values of 0 at the support. By doing this, the slab will be allowed to rotate at the support. The support conditions are shown in Figure 2.26 and 2.27. Figure 2.28 illustrates the plate and applied loading.

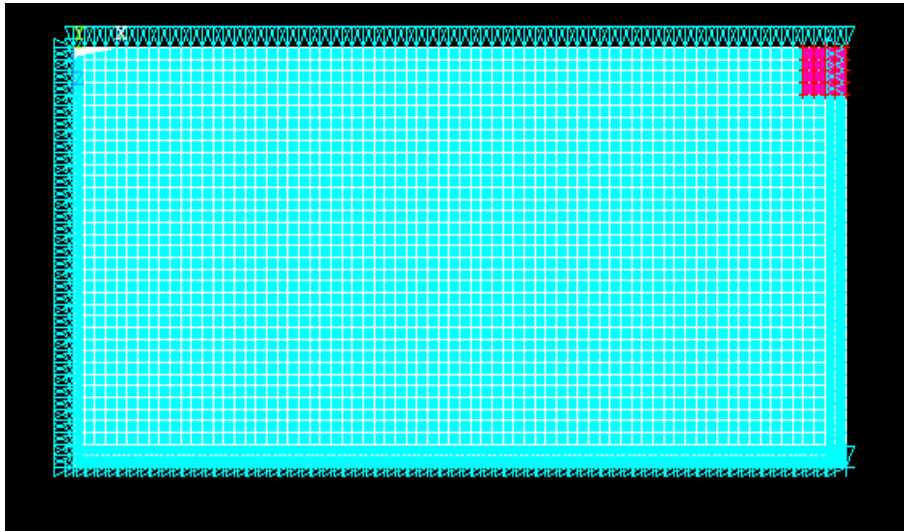


Figure 2.26: Boundary Conditions of The Slab Model

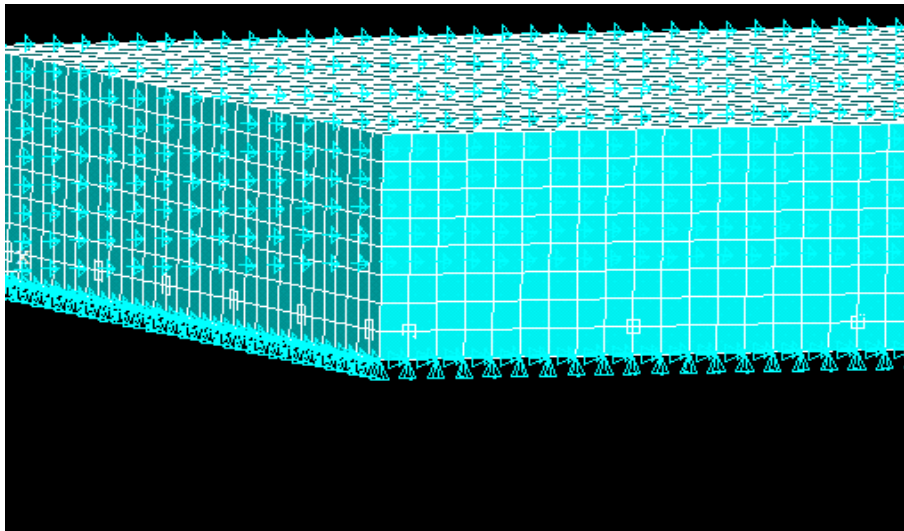


Figure 2.27: Support Conditions of The Slab Model

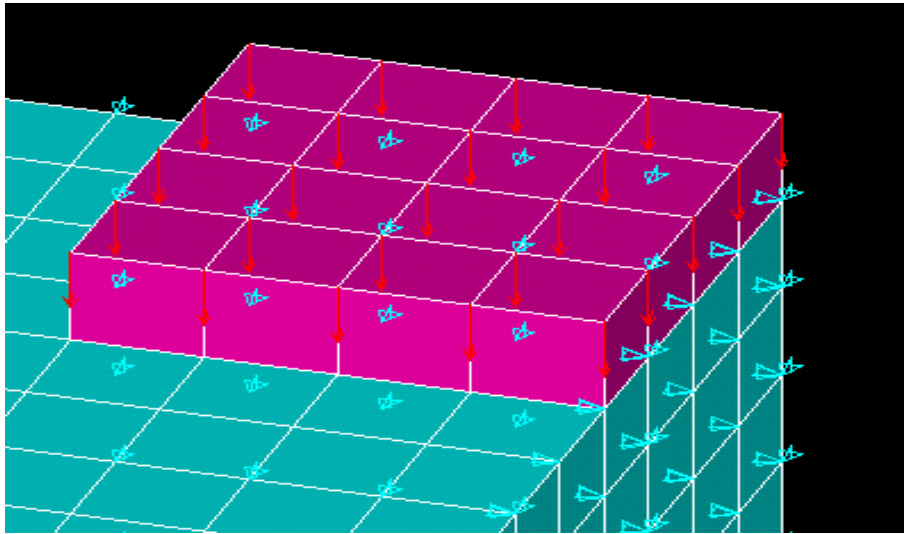


Figure 2.28: Point Loads At The Steel Plate

3 Analysis Results And Discussion

In the previous chapter we discussed how to set up the model in ANSYS with regards to material selection, element selection, real constants, geometry and meshing of the model. In this chapter we shall study how to set up the parameters for the final analysis model and look into the solution the program generates. Also a simultaneous discussion is provided on the solution of the models described in the previous chapter.

The different cases modeled using ANSYS are as follows

Beam Model I

1. Control I (reinforced Concrete Beam)
2. Notched Epoxy Beam I (reinforced concrete beam repaired with epoxy in the delaminated zone)
3. Notched Inorganic Beam I(reinforced concrete beam repaired with inorganic polymer in the delaminated zone)

Beam Model II

1. Control II (reinforced concrete beam)
2. Notched Epoxy Beam II (reinforced concrete beam repaired with epoxy in the delaminated zone)

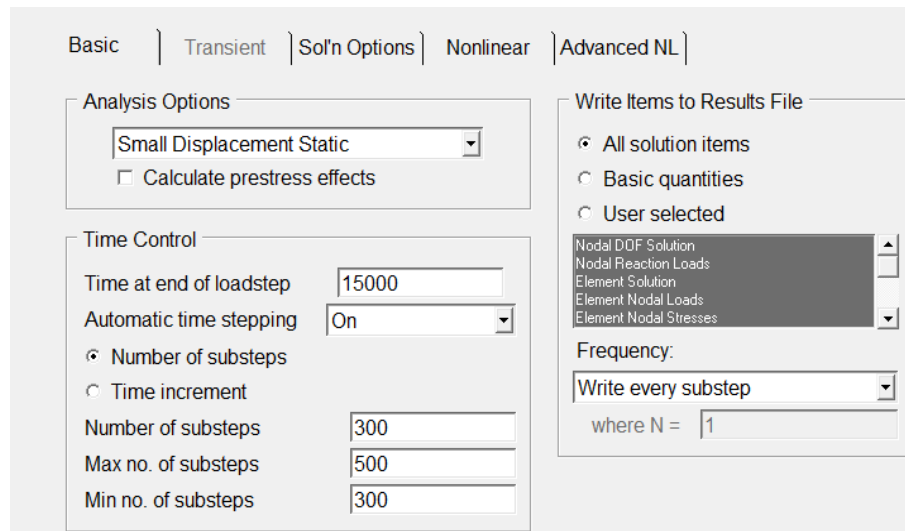
3. Notched Inorganic Beam II (reinforced concrete beam repaired with inorganic polymer in the delaminated zone)

Slab Model

1. Control Slab(reinforced concrete slab model)
2. Notched Epoxy Slab (reinforced concrete slab repaired in multiple delaminated zones with epoxy)
3. Notched Inorganic Slab (reinforced concrete slab repaired in multiple delaminated zones with inorganic polymer)
4. Notched Slab (reinforced concrete slab with delaminated zones without any repair)

3.1 Analysis

The FE analysis of the model was set up to examine three different behaviors: initial cracking of the beam, yielding of the steel reinforcement, and the strength limit state of the beam. The Newton-Raphson method of analysis was used to compute the nonlinear response. The restart command is utilized to continue the run from the last converged sub step with changes in convergence inputs till the beam completely fails. Below are the input data that are given for the analysis.



The screenshot shows the 'Nonlinear' tab of the ANSYS input dialog. The 'Analysis Options' section has 'Small Displacement Static' selected in the dropdown and 'Calculate prestress effects' unchecked. The 'Time Control' section has 'Time at end of loadstep' set to 15000, 'Automatic time stepping' set to 'On', and 'Number of substeps' selected with a value of 300. The 'Max no. of substeps' is 500 and 'Min no. of substeps' is 300. The 'Write Items to Results File' section has 'All solution items' selected, and the 'Frequency' dropdown is set to 'Write every substep' with 'where N = 1'.

Section	Parameter	Value
Analysis Options	Analysis Type	Small Displacement Static
	Calculate prestress effects	<input type="checkbox"/>
Time Control	Time at end of loadstep	15000
	Automatic time stepping	On
	Number of substeps	300
	Max no. of substeps	500
	Min no. of substeps	300
	Time increment	<input type="radio"/>
Write Items to Results File	All solution items	<input checked="" type="radio"/>
	Basic quantities	<input type="radio"/>
	User selected	<input type="radio"/>
Frequency	Write every substep	<input checked="" type="radio"/>
	where N =	1

Figure 3.1: Input Data For The Non Linear Analysis In ANSYS

In the particular case considered in this thesis the analysis is small displacement and static type. The sub steps are set to indicate load increments used for this analysis. The commands used to control the solver and output are shown in Figure 3.2.

Basic | Transient | **Sol'n Options** | Nonlinear | Advanced NL

Equation Solvers

☐ Program chosen solver

☒ Sparse direct

☐ Pre-Condition CG

Speed Accuracy

Restart Control

Number of restart files to write

Frequency:

where N =

Figure 3.2: Solution Controls

The commands used for the nonlinear algorithm and convergence criteria are shown in Figure 3.3. Values for the nonlinear algorithm were set to defaults.

Basic | Transient | Sol'n Options | **Nonlinear** | Advanced NL

Nonlinear Options

Line search

DOF solution predictor

VT Speedup

Equilibrium Iterations

Maximum number of iterations

Creep Option

☐ Include strain rate effect

Cutback Control

Limits on physical values to perform bisection:

Equiv. Plastic strain

Explicit Creep ratio

Implicit Creep ratio

Incremental displacement

Points per cycle

☒ Cutback according to predicted number of iterations

☐ Always iterate to 25 equilibrium iterations

Figure 3.3: Non Linear Solution Controls

Once the beam cracks the force convergence criteria was dropped because of non convergence, solution was based on displacement convergence criteria. The displacement tolerance was kept as low as possible to capture the correct response of the model.

3.2 Results And Discussion

As mentioned in the previous sections, a comparison is made between the experimental investigation from Klein's study(2013) and the analytical results obtained using FEA in this study. Figure 3.4 shows the load deformation curves of beams for both the studies. In the analytical model we get load deformation response till the failure of the beam, whereas in the experimental investigation the beam was loaded approximately to 60% of the maximum load. The deflection plots from experimental and analytical analysis seem to follow similar trends. The FE model deformation response is stiffer than that from the experimental results. There are several factors that may have contributed to the higher stiffness in the ANSYS FE models. Drying shrinkage and handling may produce micro cracks which may be present in concrete to some degree, these would reduce the stiffness of the actual beams, while the FE models do not include micro cracks. Perfect bond between the concrete and steel reinforcing is assumed in the FEA, but the assumption might not be true in the actual beams. As bond slip occurs, the composite action between the concrete and steel reinforcing is lost. Thus the overall stiffness of the actual beams could be lower than what the FE models predicts. In Klein's study(2013) the beam was loaded till 60% of the maximum load, then unloaded and the process was repeated for three cycles and the load deformation response was recorded. Due to the cyclical nature of the loading, the stiffness of the experimental beam could have become lower than the stiffness

of the beam modeled using FEA.

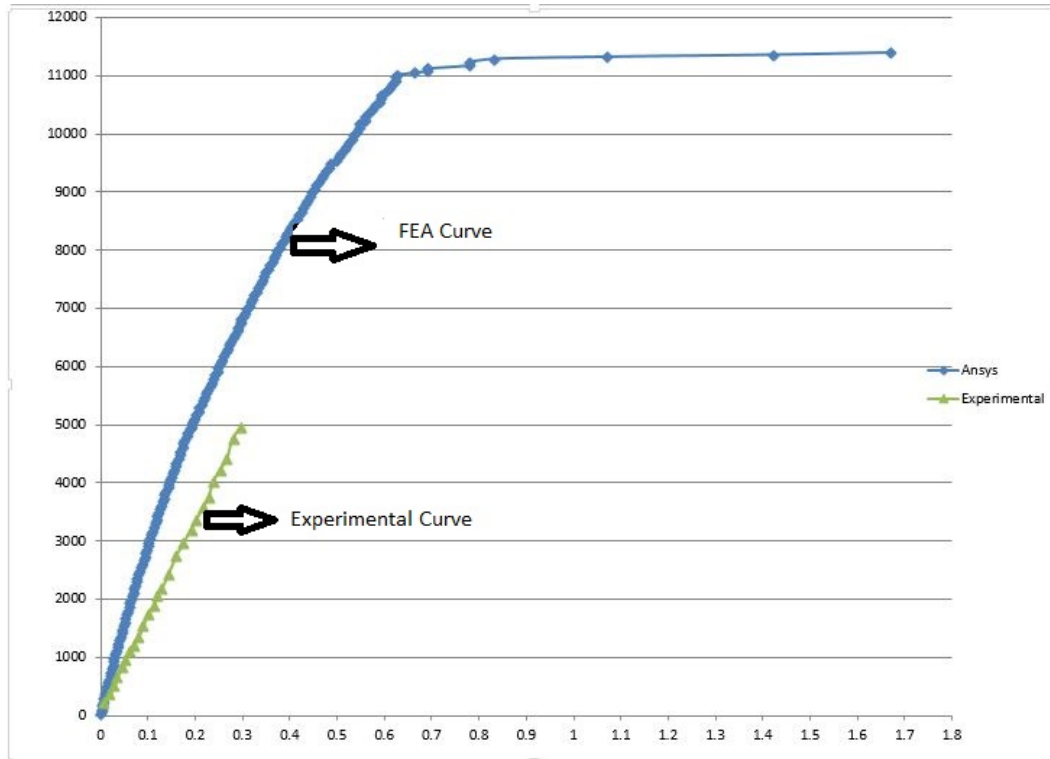


Figure 3.4: Load vs Deformation Response From Experimental and Analytical Results

3.2.1 Effect Of Bond Slip On Load vs Deformation Response Of Beams

In this section, a finite element model was developed to consider the effect of the bond slip at the interface between the rebar and concrete on beam behavior. ANSYS COMBIN39 elements were selected to simulate the bond

and bond slip at the interface between concrete and steel rebar.

COMBIN39 is a unidirectional element with nonlinear generalized force-deformation capability that can be used in most analyses. The element has longitudinal or torsional capability in one, two, or three dimensional applications. The geometry, node locations, and the coordinate system for this element are shown in Figure 3.5. The element is defined by two node points and a generalized force-deformation curve. The points on this curve (D1, F1, etc.) represent force versus relative translation for structural analyses. The force-deformation curve should be input such that deflections are increasing from the third (compression) to the first (tension) quadrants. Adjacent deformation should not be less than $1\text{E-}7$ times total input deformation range. The last input deformation must be positive. Segments tending towards vertical should be avoided. If the force-deformation curve limits are exceeded, the last defined slope is maintained, and the status remains equal to the last segment number.

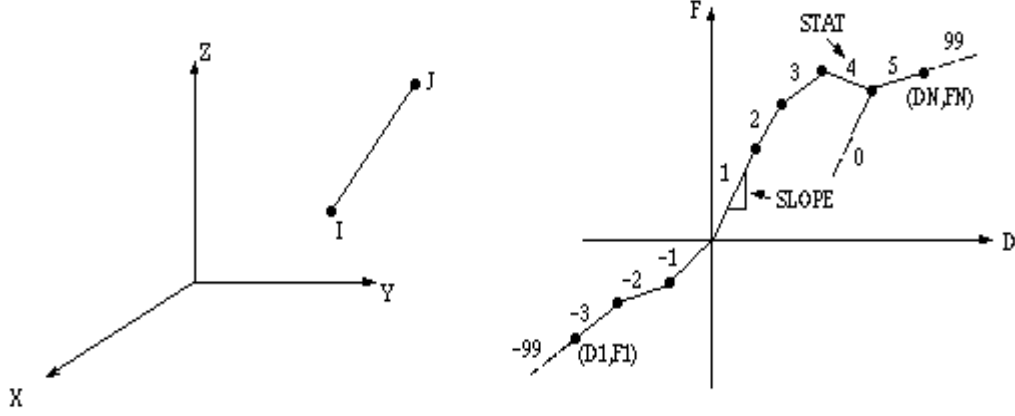


Figure 3.5: COMBIN39 Element Properties In ANSYS

The force displacement relation to be input in the model is taken from Yang and Zhu study(2012) on the investigation of effect of bond-slip properties on the load carrying capacity of corroded RC beams. The mathematical expression below relates the bond stress at the rebar location relative to the slip.

$$\tau(s) = (61.5.s - 693.s^2 + 3.14 * 10^3.s^3 - 0.478 * 10^4.s^4).f_{t,s}.\sqrt{\frac{c}{d}} \quad (3.2.1)$$

where s is the slip value(mm), c is the thickness of the cover layer(mm), d is the diameter of the reinforcement(mm) and $f_{t,s}$ is the concrete's splitting tensile strength ($\frac{N}{mm^2}$). The relationship between the bond force 'F' on a small element and slip value 's' can be calculated as follows.

$$F(s) = \tau(s).\pi.dl \quad (3.2.2)$$

Where d is the diameter of a bar(mm) and l is the distance between two adjacent springs(mm). From equation 3.2.1 and 3.2.2, the force vs displacement relationship of the spring element in the longitudinal direction can be obtained.

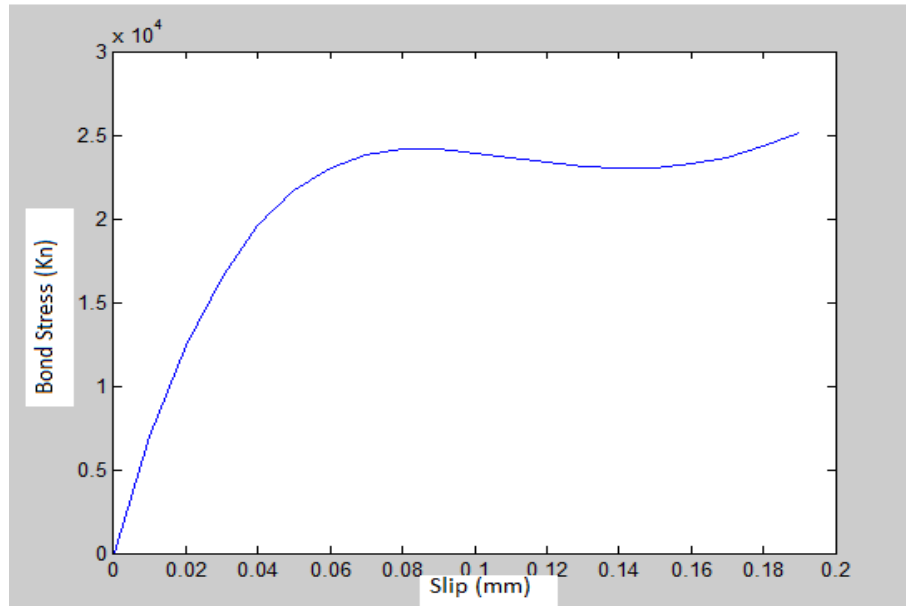


Figure 3.6: Bond-Slip Force Displacement Plot Input In ANSYS

Figure 3.6 shows the force vs displacement curve for the spring element that was input in ANSYS in the tension quadrant. For the compression quadrant the curve is a reflection of the tension curve.

In the FE model, COMBIN39 elements were modeled as zero length springs at the location where steel and concrete have shared nodes. Two sets of duplicated nodes were created at locations where steel and concrete have

shared nodes previously. Zero length springs were created such that the steel node is connected to concrete node with a spring . The zero length spring elements were defined in the longitudinal direction. The new ANSYS model includes the force displacement relation of the springs defined using the bond slip equation 3.2.1. the model was analyzed and the load deformation response of beam model I is shown in Figure 3.7.

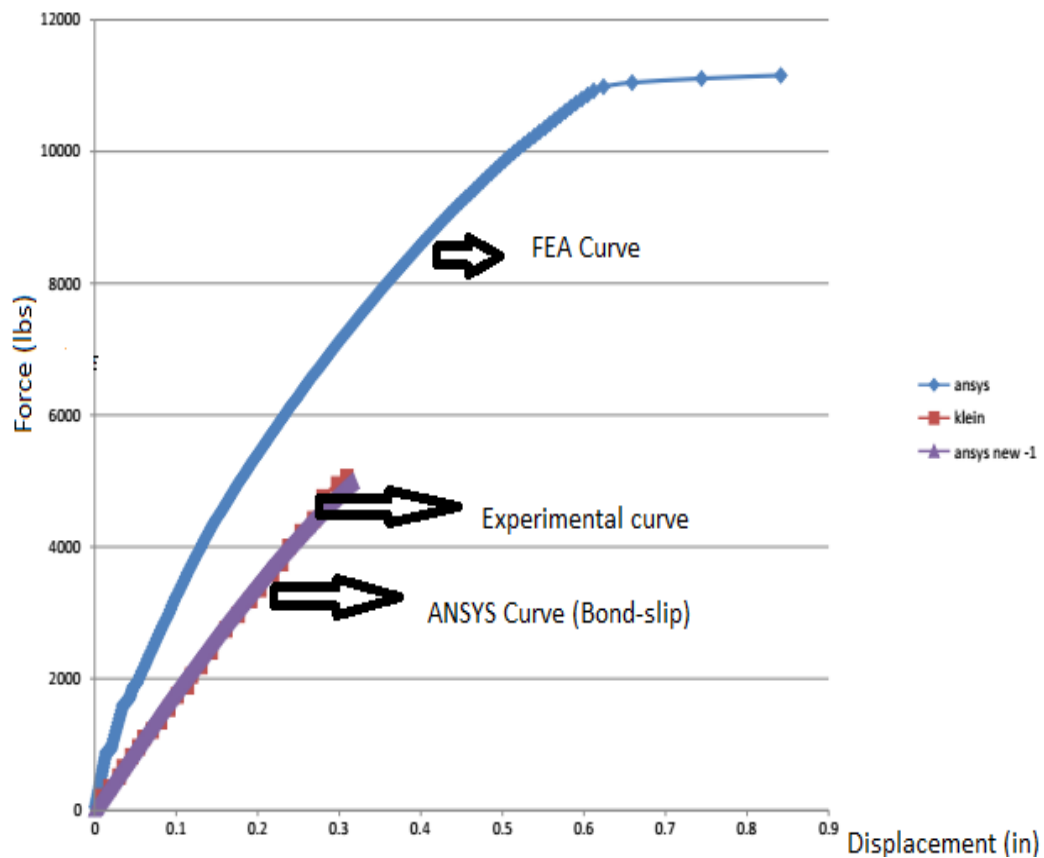


Figure 3.7: Force Displacement Response Of Various Models

Figure 3.7 shows the force deformations response for three cases. In the first case the FE model developed considers a perfect bond between the rebar and concrete and because of this assumption we observe the response of the model to load is stiffer. In the second case, a model was developed to account for the bond slip in the FE model to be compared with the experimental results which are shown in the third curve. We observe that the response of the FE model with bond slip, behaves similar to the experimental results. It can be said that incorporating the bond slip interaction at the steel concrete interface could give more accurate response of the structure, but also it should be noted that the bond slip interaction at the interface is complex to quantify and the presence of micro cracks due to handling and shrinkage, and also the cyclical nature of the loading could have caused the higher deformation to load in the experimental investigation conducted by Klein(2013).

3.2.2 Beam Model I

In this section, results for the analysis of beam model I are discussed. Cracked patterns of the beam when loaded till failure are shown in Figure 3.5,3.6 and 3.7. A cracking sign represented by a circle appears when a principal tensile stress exceeds the ultimate tensile strength of the concrete. The cracking sign appears perpendicular to the direction of the principal stress as seen in the figures below. Figure 3.5 shows a side face of a quarter beam model of control I. As shown in figure, at the bottom of the beam at mid span,

principal tensile stresses occur mostly in x direction (longitudinally). When principal stresses exceed the ultimate tensile strength of the concrete, cracking signs appear as circles perpendicular to the principal stresses in the x direction. Therefore the cracking signs shown in the figure appear as vertical straight lines occurring at the integration points of the concrete solid elements. These are also referred to as flexural cracks. In the figure below, cracking signs are observed underneath the loading locations. These cracks result from tensile strains developed due to poisson's effect (Kachlakev 2000). These cracks are referred to as compressive cracks. In the figures below, we can observe inclined cracks near the supports. These are the elements where both normal and shear stresses act. Normal tensile stresses generally develop in the x direction and shear stresses occur in the xz plane. Consequently, the direction of the tensile principal stresses becomes inclined from the horizontal. Once the principal tensile stresses exceed the ultimate tensile strength of the concrete, inclined circles appearing as straight lines perpendicular to the directions of the principal stresses appear at integration points of the concrete elements. These cracks are referred to as diagonal tensile cracks.

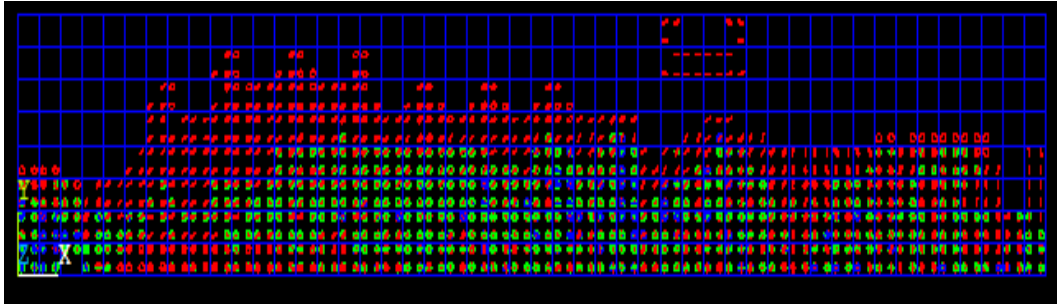


Figure 3.8: Cracked Pattern For Control I

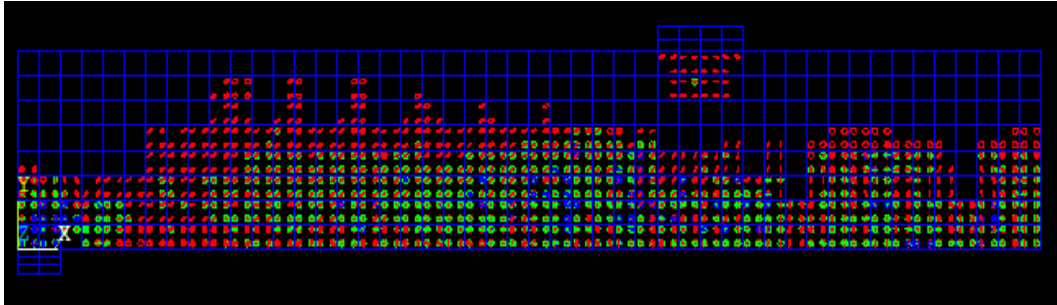


Figure 3.9: Cracked Pattern For Notched Inorganic Beam I

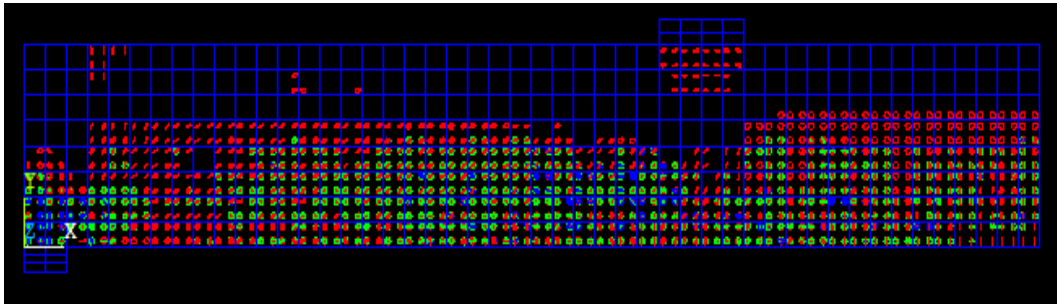


Figure 3.10: Cracked Pattern For Epoxy Beam I

Figure 3.8 to 3.10, show the stress contours for beam model I. Those figures

show the stress variation in the beam model elements for three cases modeled. Observing these figures, we can see the similarity in the stress pattern for control I and inorganic beam I. There is a continuity in stress pattern for the models, where as for epoxy beam I, the stress at the interface of the notch is very low compared to the surrounding elements. The inorganic beam I with inorganic polymer as filling material acts similar to the control I model due its comparability with concrete.

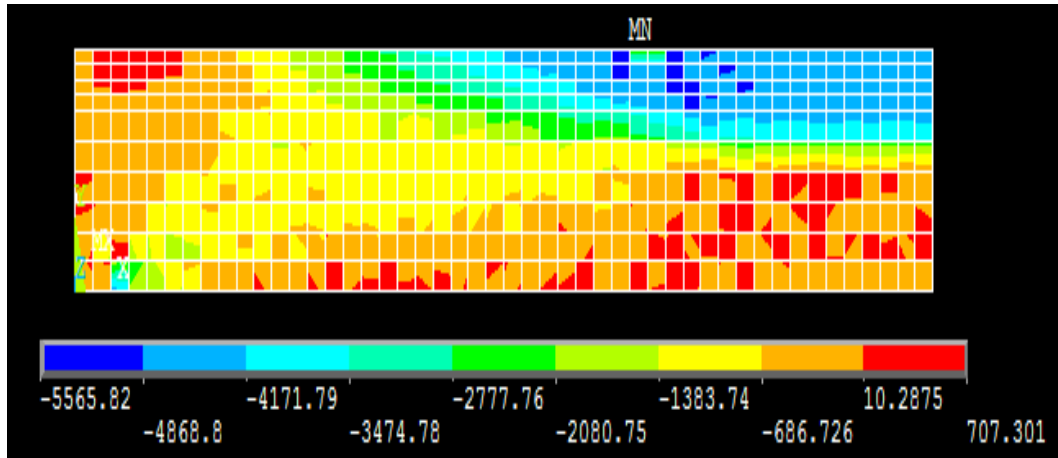


Figure 3.11: Stress Contour For Control I

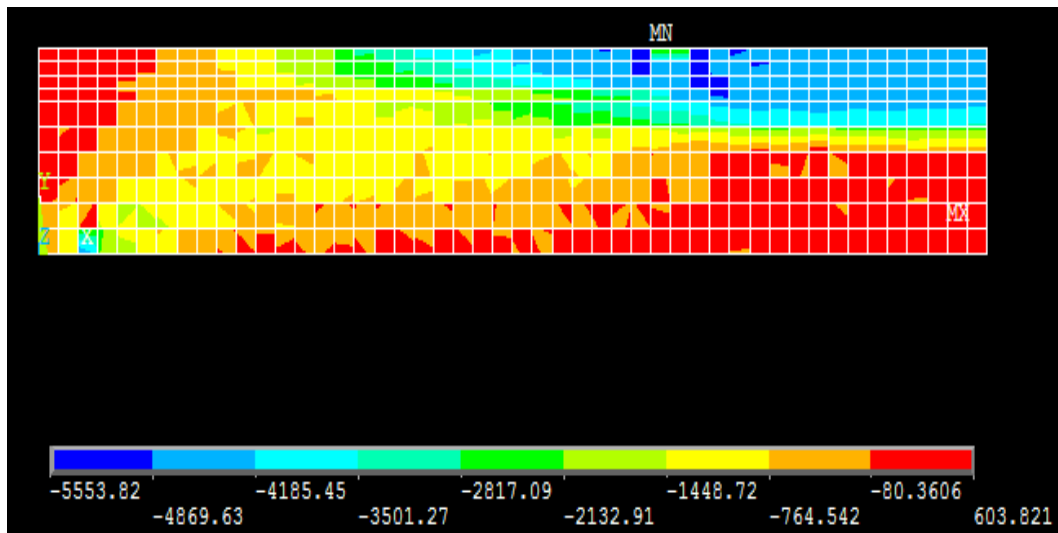


Figure 3.12: Stress Contour For Inorganic Beam I

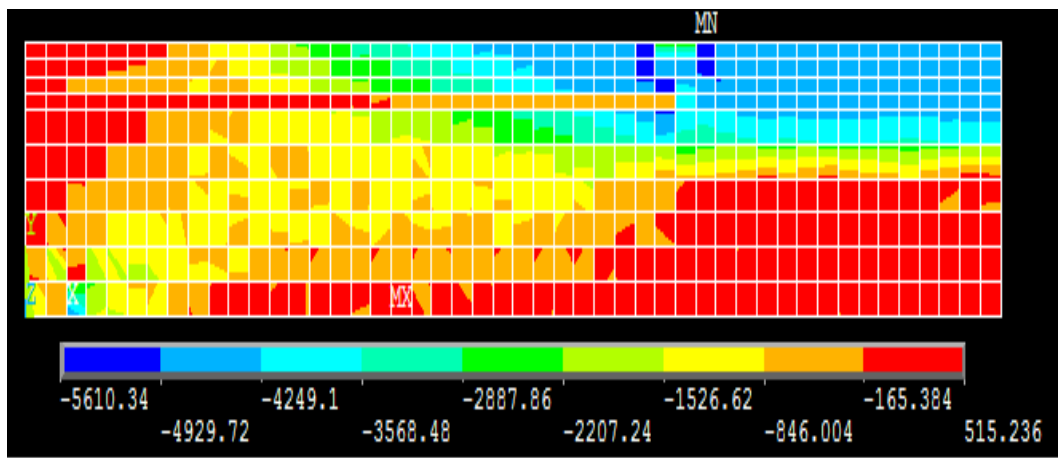


Figure 3.13: Stress Contour For Epoxy Beam I

Figure 3.11 shows a graph plotted for the elastic strain of elements at a location near the mid span of the quarter beam. The figure shows the elastic

strain along x direction over the full height of the beam.

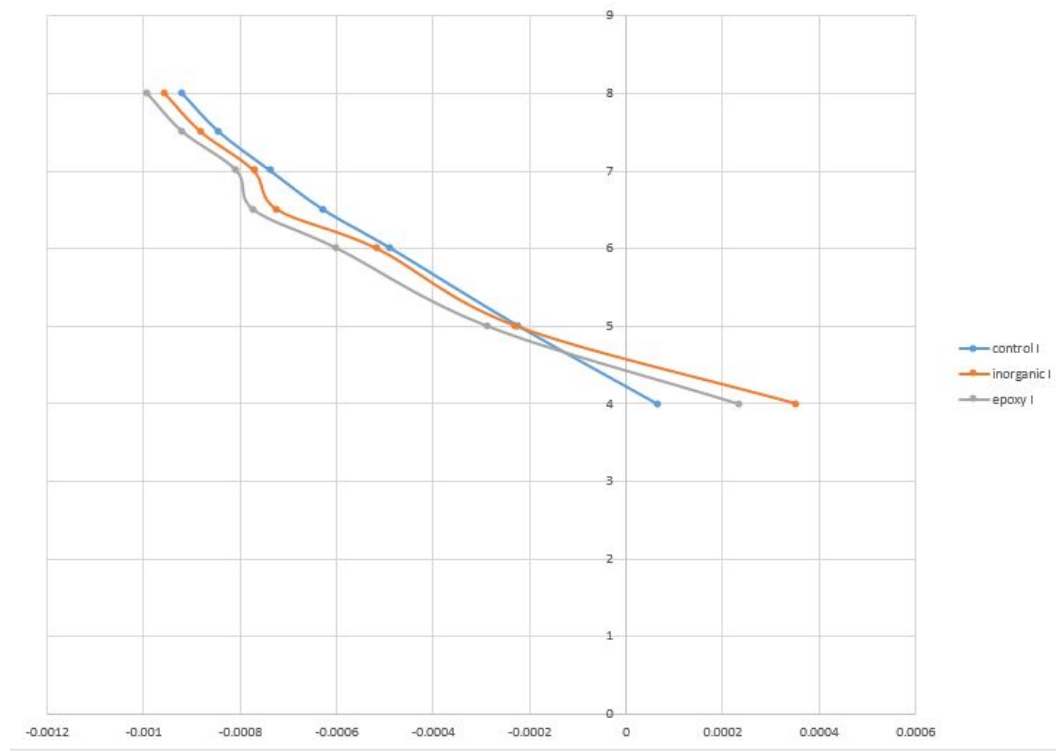


Figure 3.14: Elastic Strain Variation of FEA Models

In Figure 3.11, we can observe that the strain in epoxy I model is higher than the strain in inorganic I model, which is higher than the control model. The notch location for these models are between 6 in and 6.5 in. Due to the presence of a filling material other than concrete we can see the change in slope at this location in the strain of the elements. The epoxy I model has the highest strain along the interface. Based on the result it can be said that the inorganic polymer is a better repair material than the epoxy in concrete

applications.

Figure 3.12 shows the load displacement plot for the three cases. The displacement at the right end of the quarter beam was recorded for a node using the time history post processor tool in ANSYS. The displacement of the node at various load sub steps is stored. Similarly the force applied on the structure at various sub steps is plotted in Figure 3.12. Figure shows the force on y axis and the displacement on the x axis for the three cases modeled for beam model I.

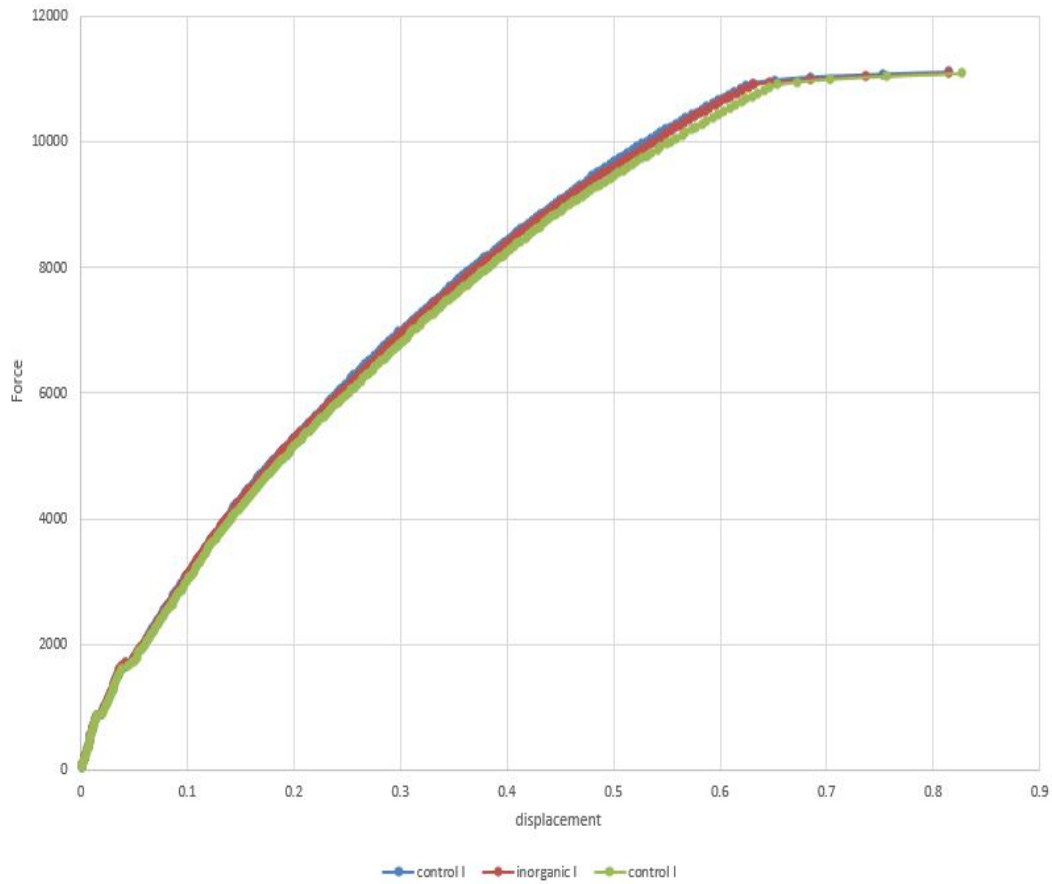


Figure 3.15: Load Displacement Plot

Looking at the load displacement plot, we can notice that the response of the structure to the load filled with repair material is very close to that of the original structure. The stiffness of the beam repaired with epoxy is slightly lower than the beam repaired with inorganic polymer. The effect of thickness of the adhesive interface on the response of the structure can be seen in the load deformation plot of beam model II, shown in Figure 3.17.

3.2.3 Beam Model II

In this section, results for the analysis of beam model II are discussed. The effect of increasing the notch thickness and the response of the structure to load is compared for the three cases modeled. The cracked pattern of the structure is similar to beam model I and is not plotted in this section. Figure 3.13 to 3.15 show the stress contours for a face of the quarter beam model in the finite elements for control II, inorganic II and epoxy II beam models.

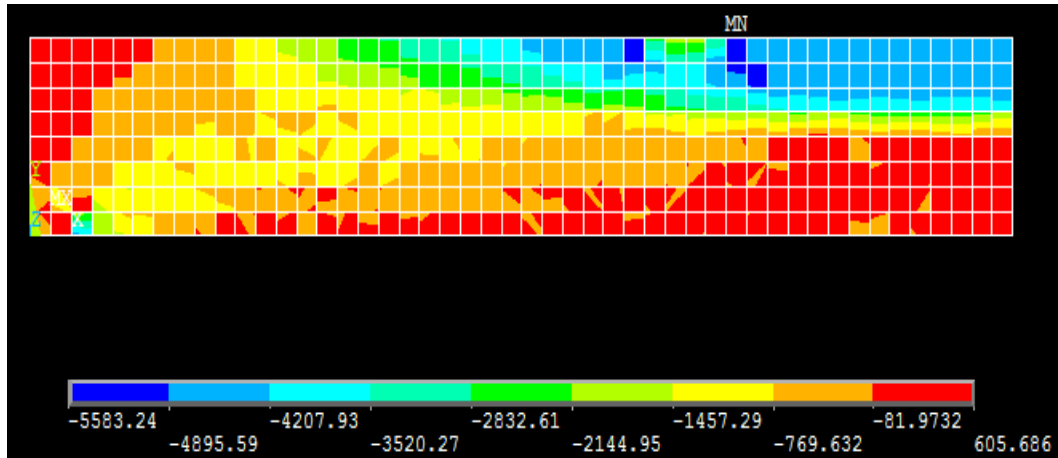


Figure 3.16: Stress Contours For Control II Model

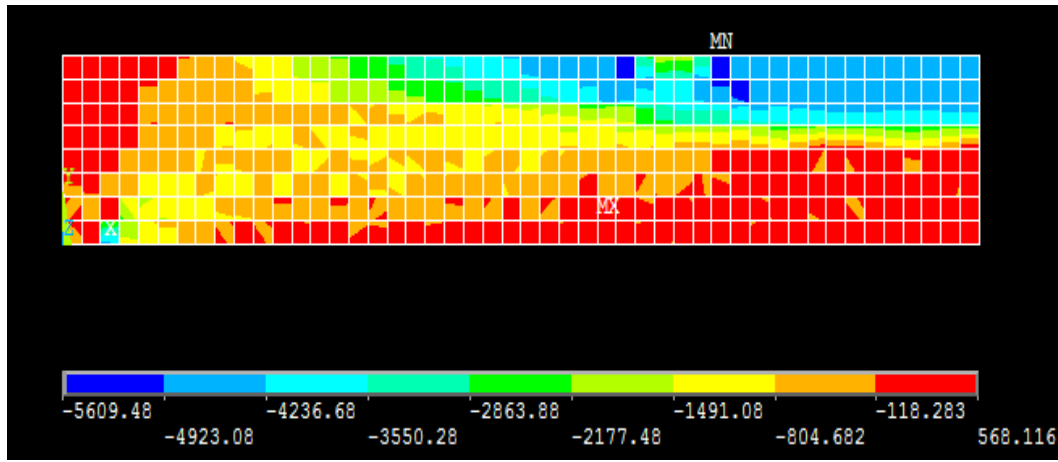


Figure 3.17: Stress Contour For Notched Inorganic Beam II Model

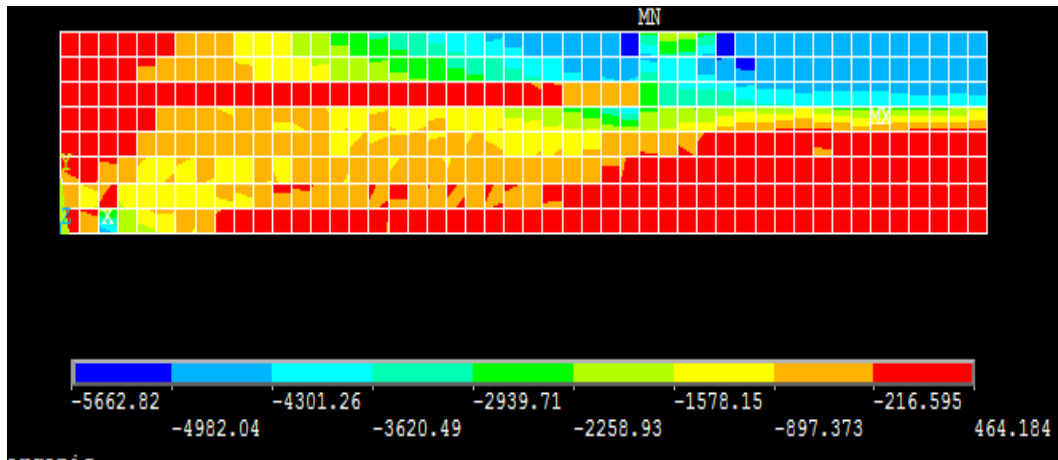


Figure 3.18: Stress Contour For Notched Epoxy Beam II Model

Similar to the beam model I, the stress contour plot for the control II model and inorganic II model show that the stresses in the finite elements are similar. The stress at the interface for the epoxy II model is very low compared

to its boundary elements. It can be said that repairing the concrete beam with inorganic polymer would make the beam almost behave like the original undamaged structure.

Figure 3.16 shows a graph plotted for the elastic strain of elements at a location near the mid span of the quarter beam. The figure shows the elastic strain along x direction over the full height of the beam for beam model II.

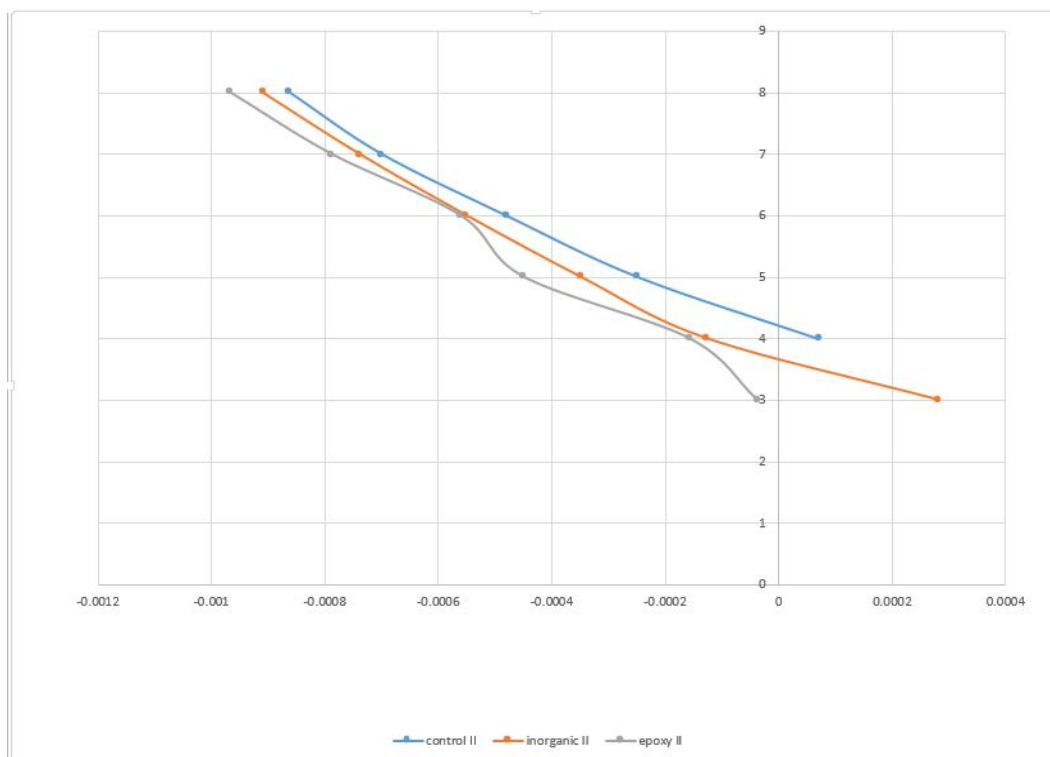


Figure 3.19: Elastic Strain Variation of Beam Model II

In Figure 3.16, the strain in epoxy II model is higher than that in the inorganic II model. The strain in control II model is lower than the other models.

The notch location to be repaired in the model is 1 inch thick located between 5 and 6 inch depth of the beam. Looking at the graph we can see the similarity in the behavior of the beam filled with inorganic polymer and the control II beam. The strain variation along the height of the cross section is uniform for both models. In the epoxy beam model II, the variation of the elastic strain is not uniform at the notch location, as we can see with the change in slope of the curve between point 5 and 6 along the y axis. It can be said that the beam repaired with inorganic polymer responds to the load applied on the structure similar to the control beam, whereas a beam repaired with epoxy might not be as compatible with concrete as the beam repaired with inorganic polymer. Comparing Figures 3.16 and 3.11, we can see the effect of thickness of the on the variation of strain along the height of the beam. It seems the thicker inorganic adhesive repair has a uniform transition at the notch location.

The graph shown in Figure 3.17 show the load displacement plot for beam model II when loaded till failure for the three cases modeled. The displacement at the end of the quarter beam was recorded using the time history post processing tool in ANSYS. Similarly the force applied on the structure is recorded for the various load steps and is plotted on the y axis, whereas the displacement is plotted on the x axis to the corresponding load step.

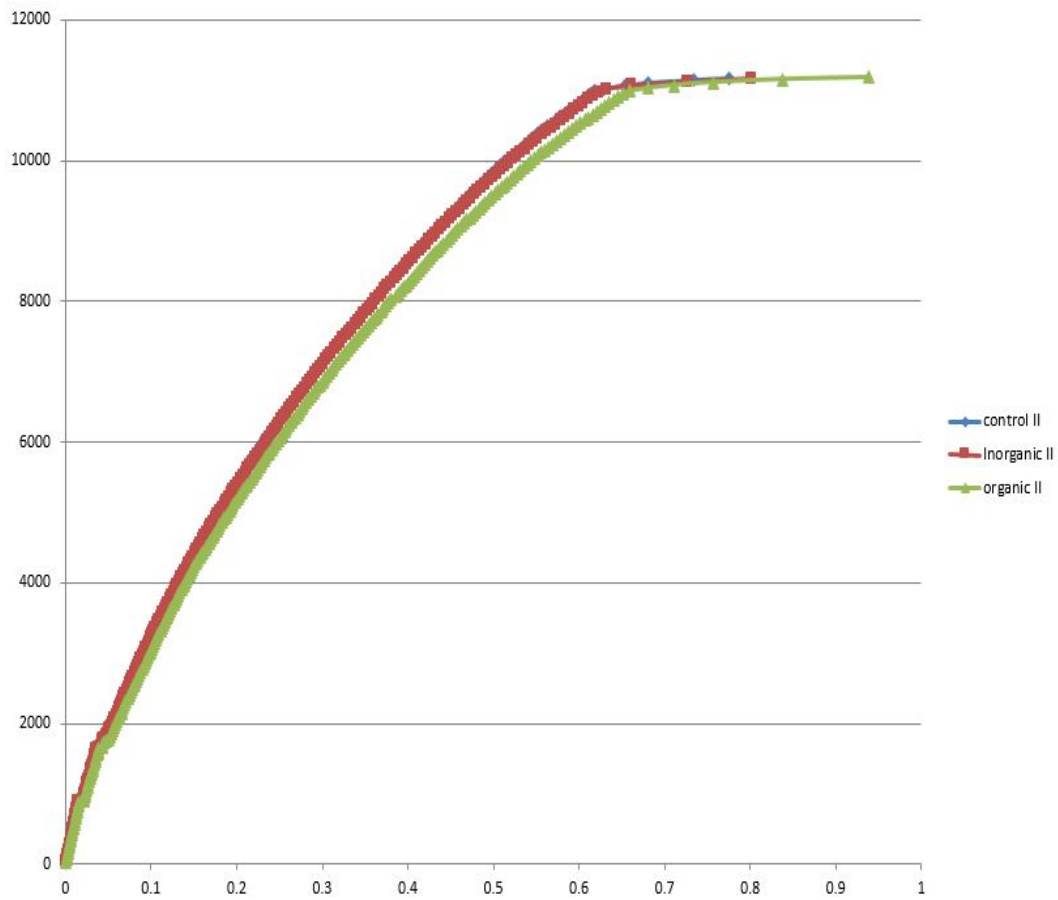


Figure 3.20: Load Displacement Plot For Beam Model II

From the graph above, the response of the inorganic beam model II to the load is similar to the control II model with the displacement being higher under failure load. For the linear range of the curve the stiffness of the both models to load is almost the same. Whereas looking at the plot for epoxy beam model II, it was noticed that the response of the beam to load was not as stiff as the other two models. Also the displacement of the structure at the

failure load is much higher in comparison. Comparing the load displacement plot for beam model I and beam model II, the increased thickness has a pronounced effect on the response of the structure to the load. A further study is conducted on the effect of varying the elastic modulus of the organic epoxy system and is reported in the appendix.

3.2.4 Slab Model

In this section, the results for the analysis of the slab model are discussed. Four FE models were developed to study the response of the slab to the applied loads. These models are 1) control case, 2) slab repaired with epoxy, 3) slab repaired with inorganic polymer and 4) fourth situation where slab is delaminated but does not have any repair material. The fourth case is modeled with elements having the properties of air at the interface for the sake of continuity and to simulate the behavior of the delaminated structure. The load displacement response is shown in Figure 3.18 to compare the various FE models. The models have three delaminated zones. These zones were used to study the response of the structure for multiple repair zones in a slab which is common practice in field application.

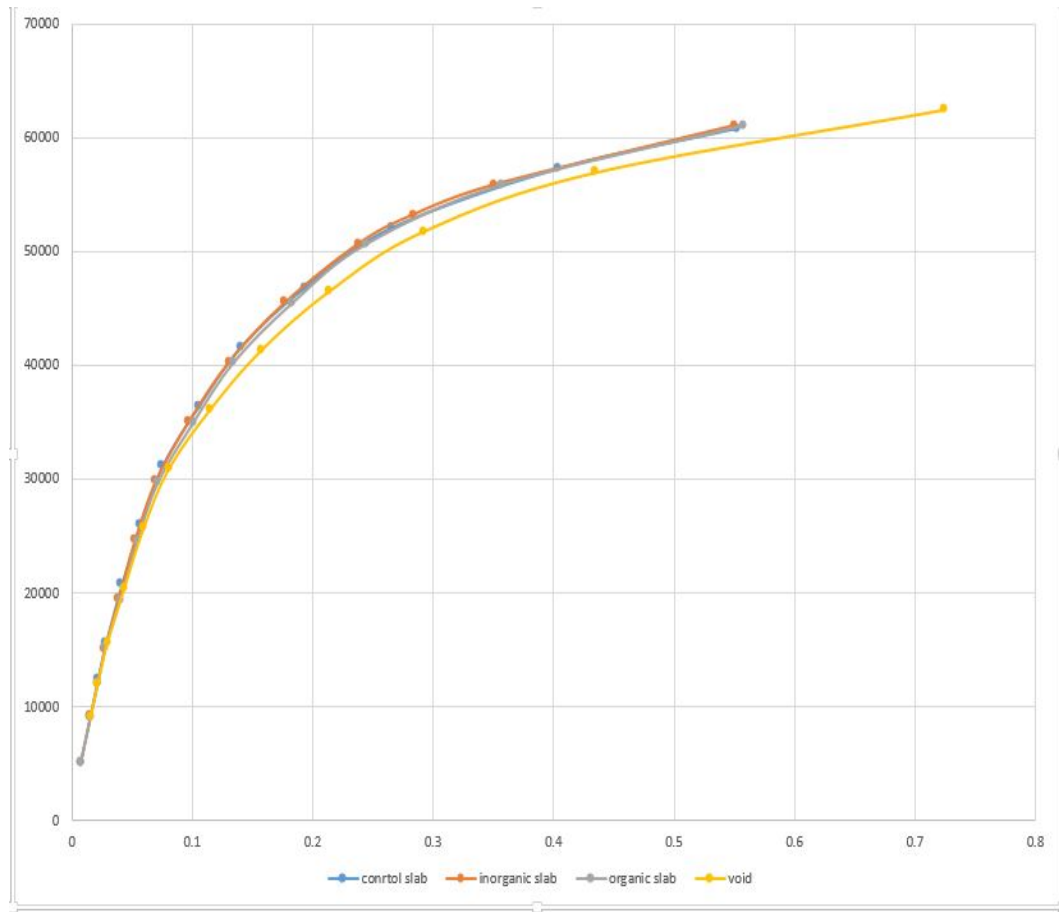


Figure 3.21: Load Displacement Plot Of Slab Model

In Figure 3.18, the displacement is plotted on the x axis and the force acting on the structure is plotted on the y axis. The response of the structure for control and slab repaired with inorganic polymer are similar. The slab repaired with epoxy comparatively has a lower stiffness than the other two models. The fourth model which contains voids in the slab has a response which is the least stiff as expected. The figure shows repairing the delami-

nated slab with epoxy or inorganic polymer is more effective and can behave in a similar way to the original structure and exhibiting similar original stiffness.

4 Conclusions and Recommendations

In the previous sections, a detail description of the model and the results obtained in this research along with a discussion were provided. Based on the results obtained in the analytical investigation the following conclusions can be drawn:

- The results of finite element based method adopted to analyze the load deformation response of repaired beams compared reasonably well with the experimental results. The finite element approach showed a slightly stiffer response than the experimental investigation. The selections of elements to model concrete, steel rebar , epoxy and inorganic polymer was validated in this model. The material laws attributed to the elements was also ascertained.
- The bond slip interaction at the steel concrete interface was included in the model and was accounted for by incorporating the bond slip relation at the interface using zero length spring elements. The results of the FE model showed similar response to the experimental results. The bond slip interaction of the steel concrete interface should be considered because of presence of micro cracks due to shrinking or cracks developed during the placement of concrete and other conditions of the interface.
- The stress at the interface or the notch location was compared for the two beam models I and II. In both models it was observed that the beam re-

paired with inorganic polymer behaved similar to the control beam, whereas the stress in epoxy material at the interface is very low compared to its surrounding elements. This seems to indicate that the inorganic polymer is more compatible with the surrounding concrete elements.

- In the two beams modeled, the beam with a 1 inch thick filler material showed considerable difference in the elastic strain along the longitudinal direction for the various filler materials. The inorganic polymer repaired beam had a higher strain but maintained the same slope throughout its height, whereas the beam repaired with epoxy had the highest strain and also there strain variation along the height of the beam was not uniform. The results showed that the inorganic polymer is more compatible with concrete than epoxy.

- The load deformation response for both the beam models with the various filler materials showed that the inorganic polymer behavior is similar to concrete, whereas the response of the beam repaired with epoxy was less stiff compared to concrete. This difference in response increased with the increase in thickness of the filler material.

- The load deformation response of the four FE slab models developed in this investigation showed the slab modeled with inorganic filler material was similar to the original slab.

Recommendations :

- Further investigation of the nature of the bond slip characteristics between the inorganic polymer and the concrete is needed. Also the nature of bond slip characteristics between epoxy and concrete needs further investigation in finite element analysis studies.
- Its common to have some inaccuracies in the structure and when loaded the defects on the tension side could increase with the tensile cracking of concrete. A study should be conducted to investigate the effects of crack propagation with a fracture mechanics based approach in ANSYS using either the VCCT approach or using cohesive zone modeling. The effect of these defects on the stiffness and capacity beams and slabs is worth further investigation.
- The elements selected in this study can be used for further applications related to finite element modeling of reinforced concrete structures. The zero length spring element used in this study to model the bond slip relation at the steel concrete interface can be used for the study of bond slip relation for two way slabs where the effect could be more pronounced.
- The inorganic polymer investigated in this study could be used as an adhesive to bond FRP to concrete structures on the tension side of the surface. A FE based approach could be adopted to investigate the response of the structure with layered solid elements for FRP, soild65 elements for concrete and adhesive, link180 elements for steel rebar. Also a bond slip interaction model could be incorporated for the slip at the interface.

References

- [1] Foden, Andrew J. 1999. *Mechanical Properties and Material Characterization of Polysialate Structural Composites*. Dissertation. New Brunswick, NJ: Rutgers, The State University of New Jersey, January.
- [2] Iowa DOT, Office of Materials. 1998. Inspection and Acceptance of Epoxy Injection Resins. Ames: Iowa Department of Transportation.
- [3] Krauss, Paul D., John M. Scanlon, Margaret A. Hanson, and Wiss, Janney, Elstner Associates, Inc. 1995. *Evaluation of Injection Materials for the Repair of Deep Cracks in Concrete Structures*. Washington, D.C.: US Army Corps of Engineers
- [4] Klein, Matthew. 2013. *Destructive repair and Rehabilitation Of Structural Elements Using High Strength Inorganic Polymer Composites*. Dissertation. New Brunswick, NJ: Rutgers, The State University of New Jersey.
- [5] Stratton, F. Wayne, Roger Alexander, and William Nolting. 1978. *Cracked Structural Concrete Repair Through Epoxy Injection and Rebar Insertion*. Final, Topeka: Kansas Department of Transportation.
- [6] Stratton, F. Wayne, and Barbara J. Smith. 1988. *Bridge Deck Hollow Plane Repair Using Injected Epoxy*. Topeka: Kansas Department of Transportation.
- [7] SealBoss. 2012. Sealboss 4040 LV Epoxy Resin. Product Data Sheet, Santa Ana: SealBoss Corporation.

- [8] Kachlakev,Damian.Miller,Thomas.*Finite Element Modeling Of Concrete Structures Strengthened With FRP laminates*.Oregon department of transportation.
- [9] William,K.J and E.P.Warnked, "*Constitutive Model for the triaxial Behavior of Concrete*",*Proceedings,International Association for Bridge and Structural Engineering*,Vol 19,ISMES,Bergamo,Italy,pp.174,1975.
- [10] Desayi,p.and S.krishnan,"Equation for the Stress-Strain curve of Concrete",*Journal of the American Concrete Institute*,61,pp.345-350,March 1964.
- [11] Wolanski,Anthony.J(2004).*Flexural Behavior of Reinforced and Prestressed Concrete Beams Using Finite Element Analysis*. Master's thesis, Milwaukee,Wisconsin.
- [12] Tavarez,F,A.,(2001) "*Simulation of Behavior of Composite Grid Reinforced Concrete Beams Using Explicit Finite Element Methods*",Master's thesis,University if Wisconsin-Madison,Wisconsin.
- [13] Yang Xiaoming,Zhu Hongqiang. "*Finite Element Investigation on Load Carrying Capacity of corroded RC Beam Based on Bond-slip*".Jordan Journal of Civil Engineering,Volume 6,No.1,2102.
- [14] Job Thomas,Ananth Ramaswamy.(2006). "*Nonlinear Analysis of Shear Dominant Prestressed Concrete Beams using ANSYS*".
- [15] ANSYS V14.5,Mechanical Users Guide, Modeling and Meshing Guide.
- [16] concreteanswers.org.

- [17] Nilson,A.H.,"*Finite Element Analysis of Reinforced Concrete Beams*",
Journal of American Concrete Institute,65(9),pp.757-766,1998.
- [18] Bangash,M.Y.H.,*Concrete and Concrete Structures:Numerical Modeling
and Applications*, Elsevier Science Publishers Ltd.,London,England,1989.

A Appendix

A.1 Comparison Between Full Volume Model and Quarter Volume Model

In this section the study conducted to evaluate and compare the response of the quarter volume and full volume model of the structure is reported. A FE model was developed to consider the difference in response between the quarter volume model and the full beam model. A full volume model was developed maintaining the same mesh density, same material input data and same solution controls for the analysis. The load vs deformation response of the structure is plotted in fig A.3.

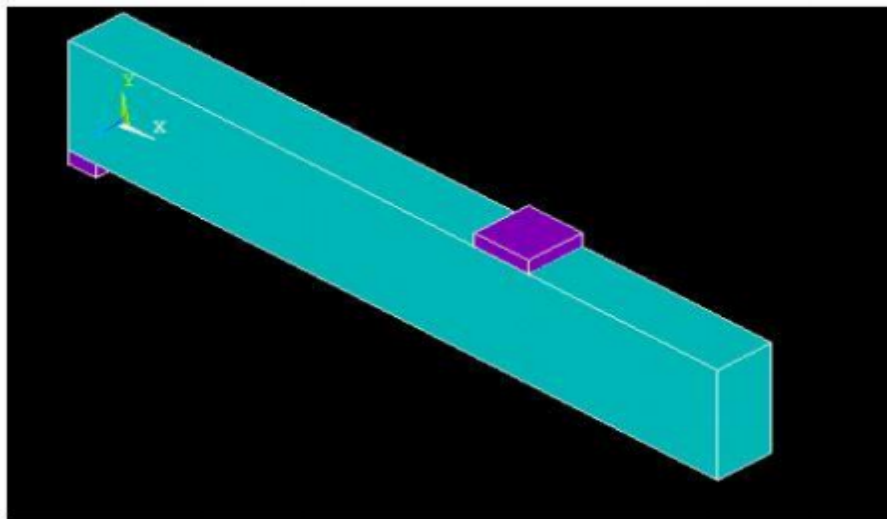


Figure A.1: Quarter Volume Model

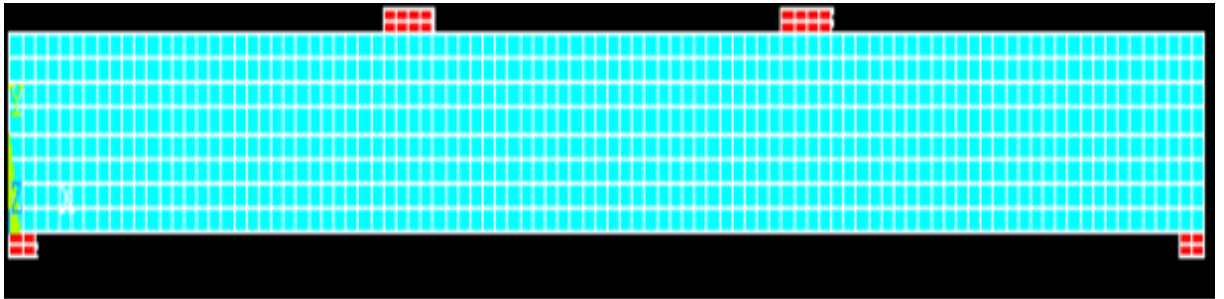


Figure A.2: Full Volume Model

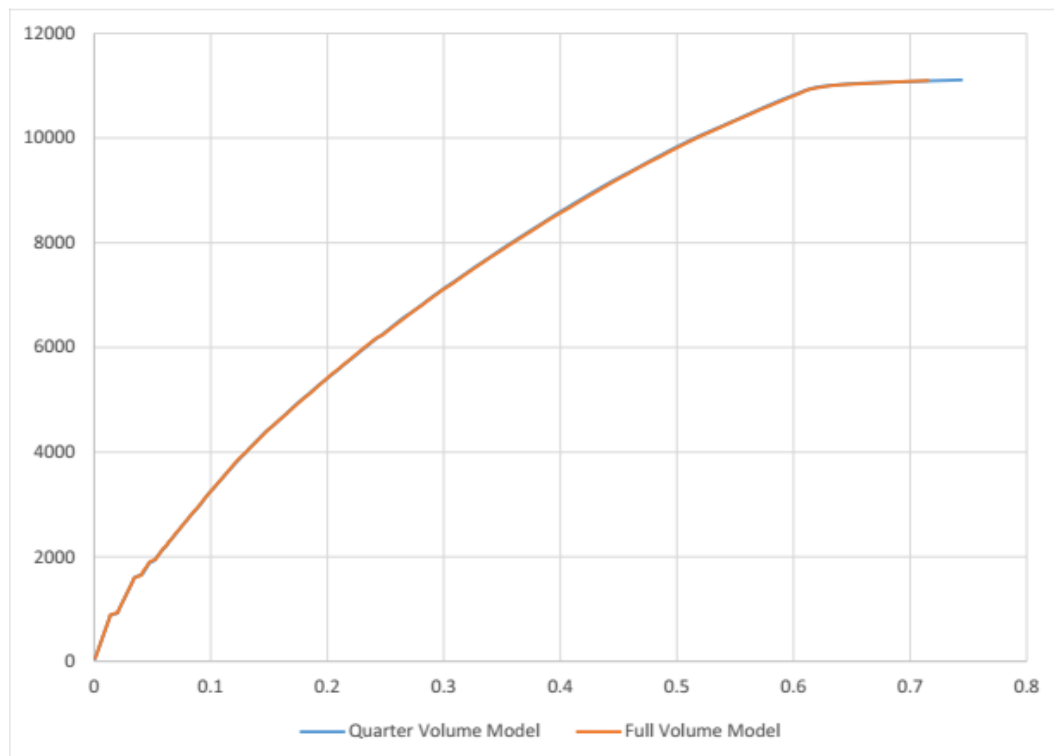


Figure A.3: Load Deformation Response from Quarter and Full Beams Models

Observing the load deformation response for both the models in fig A.3., it is observed the quarter volume model with symmetry boundary condition has an identical response to the full beam model. The FE models in this study were quarter volume mesh, taking advantage of the symmetry to reduce computational time.

A.2 Effect of Elastic Modulus of Filler Material on Stiffness

A FEM model was developed with a refined mesh at the interface location to capture better response of the structure.

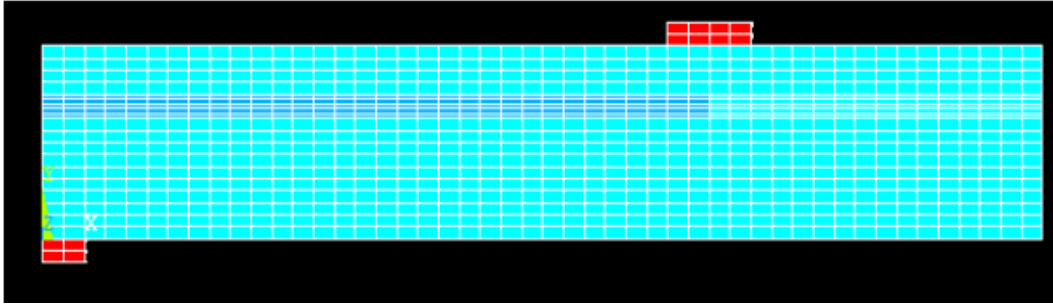


Figure A.4: Refined FE Mesh for Repaired Beam

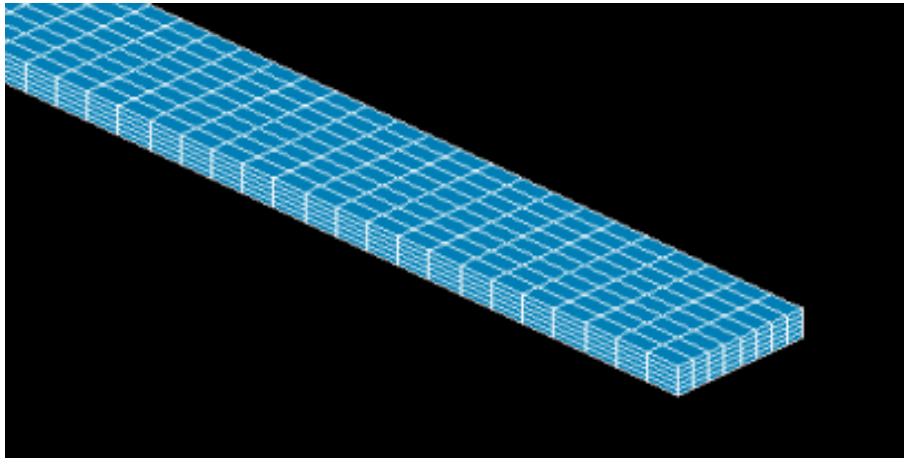


Figure A.5: Refined FE Mesh for Filler Region

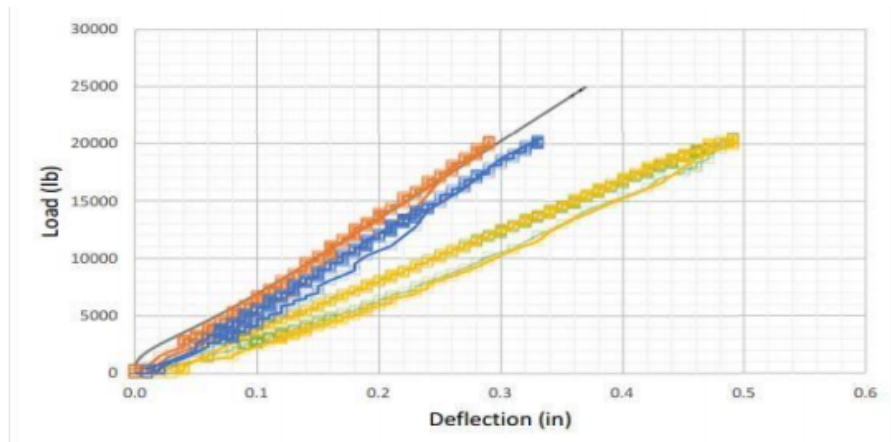


Figure A.6: Load Deformation Response, Organic Epoxy (yellow), Notched Beam (Green), Control Model (Blue), Inorganic Polymer (Orange)

Fig A.6., shows the load deformation response of the various cases of beams tested by Klein (2013) in his experimental investigation. Observing this

figure, it can be seen that the response of the beam repaired with epoxy and the case where the beam is notched without any repair material have a similar response. This suggests that the epoxy was not effective in restoring the stiffness of the beam due to material incompatibility. This seems to suggest the elastic modulus of the organic epoxy is very low compared to concrete or the inorganic filler. The elastic modulus of epoxy can vary depends on several factors such as composition, temperature, method of application and can be lower than the value specified in the product sheet. To evaluate the effect of the variable elastic modulus of epoxy, a FE analysis was conducted on the response of the beam repaired with epoxy for varying elastic moduli. Fig A.7., shows the load deformation response of the control model, the model of beam repaired with inorganic polymer, and the model of beam repaired with epoxy with varying elastic moduli.

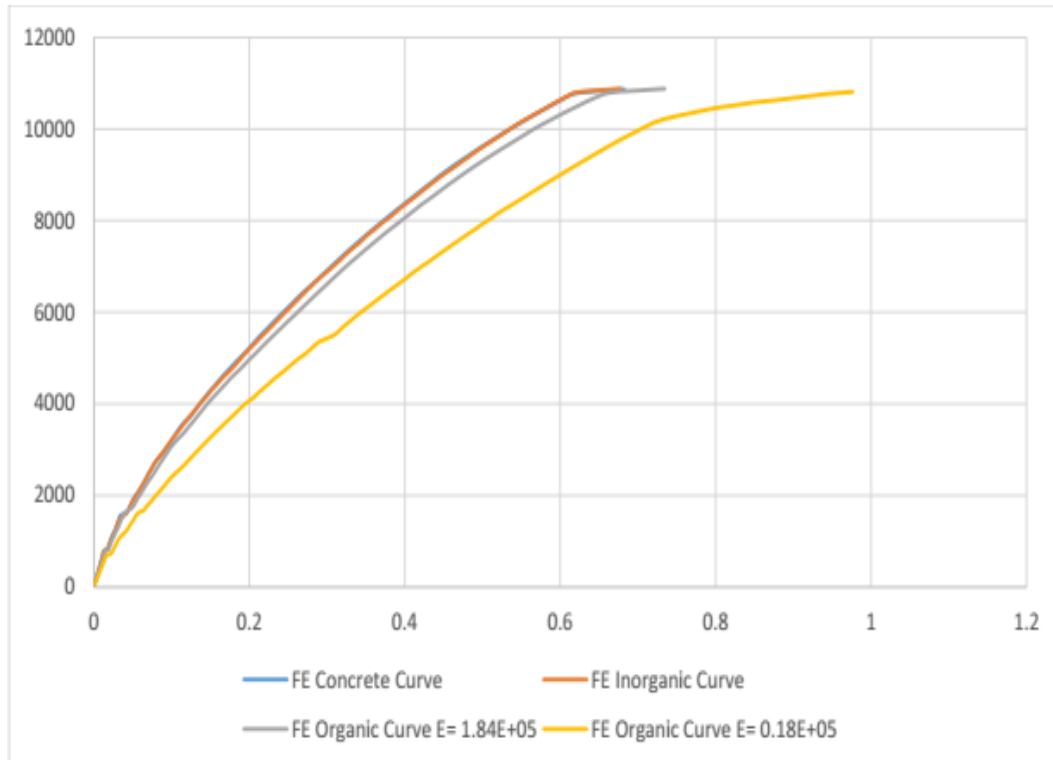


Figure A.7: Load Deformation Response from FE Models for Various Cases

Observing the load deformation response in fig A.7., it is observed that the load deformation response of the beam repaired with organic epoxy with an elastic modulus of $0.18\text{E}+05$ psi has the least stiffness as expected. The figure also shows considerable difference in stiffness compared to the beam repaired with organic epoxy but with higher modulus.

A.3 Effect of Shear Retention

The tensile cracking which occurs in concrete is generally modeled in FEA by two approaches. In the first approach which is known as discrete element method, the cracks developed in the concrete are locally modeled in this approach. Separation between adjacent elements representing the crack has to be accurately modeled. The limitation of this method is that one needs to know the cracking path prior to performing FE analysis. Initial meshing should comply with this path and also the FE mesh needs to be regenerated at every crack-propagation step. This makes this analysis time-consuming and expensive.

The alternative method assumes a smeared crack approach which considers fracture distribution over damaged region. So, this geometrical nonlinearity may be simulated with material stiffness degradation while crack propagation occurs. This option of concrete modeling can be selected by modeling the structure with SOLID65 element available in ANSYS. SOLID65 is modeled as a 3D solid with 8 nodes. This element is a linear order element, which might be overly stiff in bending dominated problems. Higher order displacement response cannot be assigned to this element, this is one of the limitation of the SOLID65 element.

Shear transfer coefficient which needs to be input for the concrete model varies from 0.0 to 1.0, with 0.0 representing a smooth crack (complete loss of shear transfer) and 1.0 representing a rough crack (no loss of shear transfer).

This specification may be made for both the closed and open crack. A shear transfer coefficient of 0.3 was adopted in the study, choosing an appropriate factor for shear transfer coefficient is very important. Improper selection of the factor might lead to shear locking leading to stiffer elements.

To evaluate the effect of the shear retention factor on the load deformation response, several FE models were developed for variable values of the shear retention factors. Fig A.8., shows the load deformation response of the FE models with varying shear retention factor for open crack. These FE plots are compared to the experimental load deformation response from Klein (2013).

The assumptions made in FE models were the following:

- Concrete is cracked before the load was applied (tensile strength 10 psi).
- Inorganic polymer was given a tensile strength of 530 psi (not cracked initially).
- Elastic modulus of organic epoxy was taken as 1E+05 psi.
- A higher displacement convergence criteria of 0.025 compared to 0.005 was given for concrete with shear coefficient 0.01 for the sake convergence. (displacement convergence criteria = $U_{i+1} - U_i < \text{Value Specified}$)

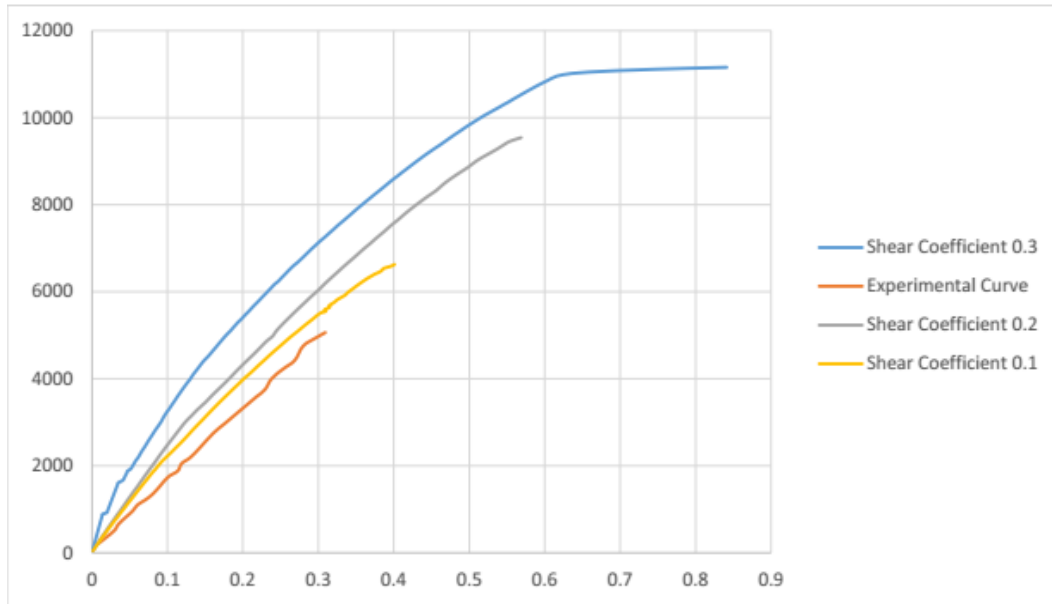


Figure A.8: Load Deformation Response for the Concrete Model

Observing the load deformation response for the various cases, it is seen that concrete with a shear retention factor of 0.3 was the stiffest and had the highest failure load with the steel yielding before compression failure. The model with a shear retention value of 0.1 was least stiff and was comparable to the response of the experimental beam but failed at a much lower load compared to the beam with a shear coefficient of 0.3.

The load deformation response for the beams repaired with inorganic polymer and with organic epoxy with a shear coefficient of 0.1 and 0.3 for open crack in concrete is also plotted in figures A.9., and A.10., respectively. The load deformation response of the repaired beams also show that the beam is stiffer

when the shear retention factor is higher.

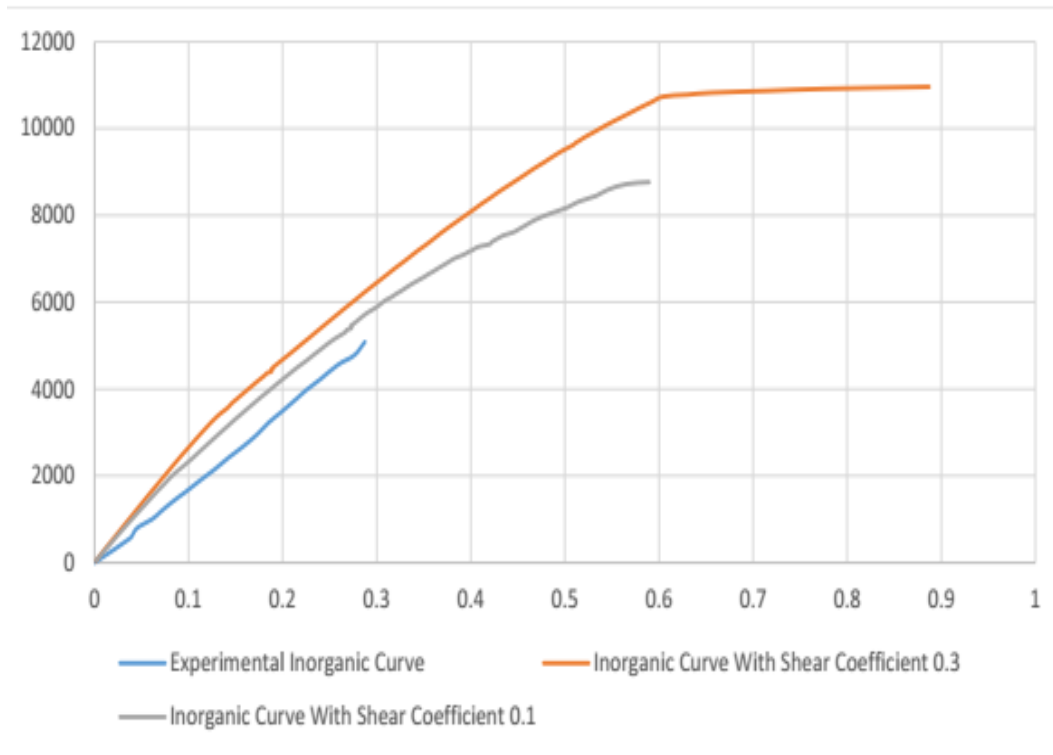


Figure A.9: Load Deformation Response for Beam Repaired with Inorganic Polymer for Various Shear retention 0.1 and 0.3

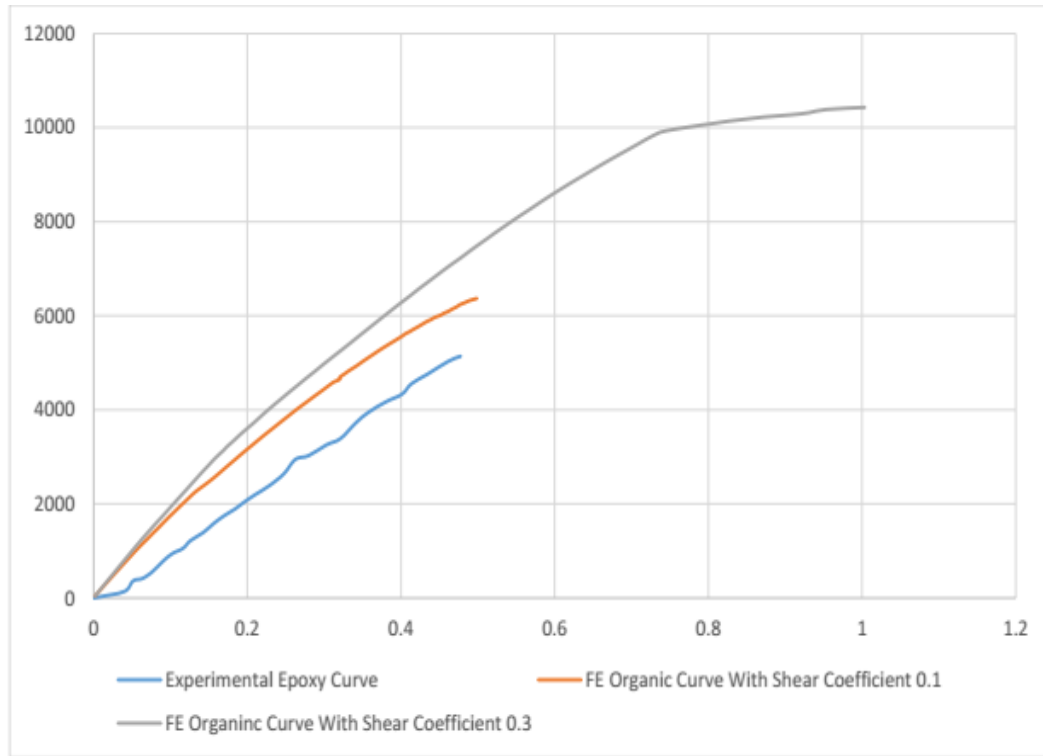


Figure A.10: Load Deformation Response for Beam Repaired with Organic Epoxy for Various Shear retention 0.1 and 0.3

Conclusion

The FE study of reinforced concrete is complex due to the nature of the material. In finite element modeling of reinforced concrete beams, there are various factors that affect load deformation response of the beam such as the shear retention factor, the mesh density, the bond-slip interaction at the steel concrete interface and also the approach to crack modeling due to cracking

in tension. Employing Newton-Raphson method for non-linear analysis also has its limitation as concrete has to be modeled as perfectly plastic after reaching its maximum stress. General FE purpose programs such as ANSYS may be used to evaluate the response of reinforced concrete beams but has its limitations.